

# Fully Discrete Positivity-Preserving and Energy-Decaying Schemes for Aggregation-Diffusion Equations with a Gradient Flow Structure

Rafael Bailo\*, Jose A. Carrillo† and Jingwei Hu‡

September 3, 2022

## Abstract

We propose fully discrete, implicit-in-time finite volume schemes for general nonlinear nonlocal Fokker-Planck type equations with a gradient flow structure, usually referred to as aggregation-diffusion equations, in any dimension. The schemes enjoy the positivity-preserving and energy-decaying properties, essential for their practical use. The first order in time and space scheme unconditionally verifies these properties for general nonlinear diffusion and interaction potentials while the second order scheme does so provided a CFL condition holds. Dimensional splitting allows for the construction of these schemes with the same properties and a reduced computational cost in higher dimensions. Numerical experiments validate the schemes and show their ability to handle complicated phenomena in aggregation-diffusion equations such as free boundaries, metastability, merging and phase transitions.

**Key words.** gradient flows, implicit-in-time schemes, fully discrete finite volume schemes, positivity-preserving, energy-decaying.

## 1 Introduction

In this work we consider the following family of nonlinear nonlocal aggregation-diffusion equations

$$\begin{cases} \rho_t = \nabla \cdot [\rho \nabla (H'(\rho) + V + W * \rho)], & \mathbf{x} \in \mathbb{R}^d, t > 0, \\ \rho(\mathbf{x}, 0) = \rho_0(\mathbf{x}), \end{cases} \quad (1.1)$$

where  $\rho = \rho(\mathbf{x}, t) \geq 0$  is the unknown particle density,  $H(\rho)$  is the density of internal energy,  $V(\mathbf{x})$  is the confinement potential, and  $W(\mathbf{x})$  is the so-called interaction potential, see [33, 59] for instance. By definition  $H$  is a convex function in order for the first term  $\nabla \cdot (\rho H''(\rho) \nabla \rho)$  to be a (possibly degenerate) nonlinear density dependent diffusion. The drift terms  $\nabla \cdot [\rho \nabla (V + W * \rho)]$  correspond to forces acting on the particles given by external sources  $V(\mathbf{x})$  and attractive-repulsive forces between particles with potential  $W(\mathbf{x})$ .

These equations can be derived as mean-field limits of particle systems or as an upscaling of cellular automata with applications in granular materials [7, 6], cell migration and chemotaxis [14, 18, 47, 23], collective motion of animals (swarming) [55, 46, 28], opinion formation [48, 41], self-assembly of nanoparticles [44], and mathematical finance [40] among others. In the particular case of linear diffusion, these

\*Department of Mathematics, Imperial College London, SW7 2AZ London, UK (r.bailo@imperial.ac.uk).

†Department of Mathematics, Imperial College London, SW7 2AZ London, UK (carrillo@imperial.ac.uk).

‡Department of Mathematics, Purdue University, West Lafayette, IN 47907, USA (jingwei@purdue.edu).

models correspond to macroscopic limits of interacting particle systems in terms of Fokker-Planck type equations, see for instance [54, 11] and the references therein. They lead to interesting evolutionary phenomena such as noise induced phase transitions and metastability behavior [4, 42, 5], present too in nonlinear diffusion type models [16, 20, 23]. Typical interaction potentials  $W(\mathbf{x})$  appearing in the applications are radial and can be fully attractive such as the Newtonian or Bessel potentials in chemotaxis [23] or power-laws in granular materials [33]; repulsive in the short range and attractive in the long range such as combinations of power-law potentials or Morse-type potentials in swarming [55, 32]; or compactly supported potentials in many biological applications such as networks and cell sorting [5, 21].

The equation (1.1) possesses interesting properties. First, its solution should always be a nonnegative density. Second, it has a variational structure: it is a gradient flow of the free energy functional as discovered in [33]. More precisely, defining the free energy functional

$$E(\rho) = \int_{\mathbb{R}^d} \left[ H(\rho) + V\rho + \frac{1}{2}(W * \rho)\rho \right] d\mathbf{x},$$

then its formal variation for zero mass perturbations is given by  $\xi := \frac{\delta E}{\delta \rho} = H'(\rho) + V + W * \rho$ , and then the evolution of the free energy along a solution of (1.1) is given by

$$\frac{dE}{dt} = \int_{\mathbb{R}^d} \frac{\delta E}{\delta \rho} \frac{\partial \rho}{\partial t} d\mathbf{x} = \int_{\mathbb{R}^d} \xi \nabla \cdot [\rho \nabla \xi] d\mathbf{x} = - \int_{\mathbb{R}^d} \rho |\nabla \xi|^2 d\mathbf{x} \leq 0. \quad (1.2)$$

This dissipation property has another interpretation; namely the solution to (1.1) is the gradient flow or the curve of steepest descent for the free energy functional  $E$  in the sense of the euclidean transport distance between probability measures as discussed in [2, 33, 23] and the references therein. It is important to notice that this dissipation property entails a full characterisation of the set of stationary states: they are given by nonnegative densities such that  $\xi$  is constant (possibly different) in each connected component of their support. Therefore, the free energy is a Liapunov functional for (1.1) and useful to discuss the stability of the equilibria in many particular cases, see [33, 30]. Let us point out that these properties persist when solving this equation in a bounded domain  $\Omega$  with no-flux boundary conditions, provided the convolution is understood by extending the density by zero outside  $\Omega$  and  $\nabla \xi \cdot \eta(x) = 0$  is satisfied for all  $x \in \partial\Omega$ , where  $\eta(x)$  is the outwards unit normal vector to the boundary of  $\Omega$ .

These nonlinear Fokker-Planck equations have been the center of much attention by the numerical analysis and simulation community in the last years. In fact, a central question has been to design numerical schemes capable of preserving the structural properties of the gradient flow equation (1.1) such as nonnegativity, the dissipation property (1.2), and a corresponding discrete set of stationary states approximating accurately the long time asymptotics of these equations. First and second order accurate finite volumes schemes which treat (1.1) as a nonlinear continuity equation with a vector field given by  $-\nabla \xi$  were proposed in [8, 20] for nonlinear diffusions and aggregation-diffusion equations respectively. They enjoy the semidiscrete (in space) entropy dissipation property and positivity preserving for the explicit-in-time discretisation under a CFL time step restriction. A generalisation of these ideas for high order approximations using a discontinuous Galerkin approach have been proposed in [53] with a suitable high order quadrature rule using Gauss-Lobato formulas.

In the case of linear diffusions, schemes enjoying the semidiscrete free energy dissipation were known in granular media Fokker-Planck equations [12, 13] based on the Chang-cooper discretisation approach [36]. Such schemes have been generalised and improved for equations of the form (1.1) in [50] leading to second order accurate finite difference schemes with a semidiscrete entropy dissipation property again. Linear Fokker-Planck equations have plenty of other entropies, and spectral schemes were used in [43] to have a decay of the weighted  $L^2$  entropies. Finally, implicit-in-time semidiscretisations were proposed in [3, 29] having the discrete-in-time free energy decay for nonlinear Fokker-Planck equations of the form (1.1) with  $W = 0$ . These schemes are reminiscent to convex splitting ideas in the variational  $L^2$  framework as developed in [52], however they are not directly applicable in the setting of gradient flows with respect to measures. Other numerical schemes used for nonlinear Fokker-Planck equations include finite element schemes [15], particle/blob methods [38, 19, 22], and methods based on the gradient flow formulation in terms of steepest descents with euclidean transport distances [10, 34, 49, 45, 35, 27].

In a recent work [1] the authors have proposed several fully discrete implicit-in-time discretisations for the Keller-Segel model in one dimension with linear diffusion and nonlinear chemosensitivity allowing for the energy decaying property. Among them, they presented an implicit-in-time fully discrete scheme based on the gradient flow ideas in [16, 20, 53]. In the present work we generalise these ideas proposing fully discrete (both in space and in time) implicit finite volume schemes for equation (1.1) that are both positivity-preserving and energy-decaying; these properties are met unconditionally by a scheme with first order accuracy in time and space, and met under a parabolic CFL condition by a second order in space scheme. Both schemes work for general nonlinear diffusions and general interaction potentials  $W$  through a careful combination of the implicit-in-time discretisations as hinted in [1]. Special care has to be taken in using the implicit schemes as the Jacobian matrix can be ill-conditioned in the presence of vacuum due to the nonlinear diffusion terms. A detailed study of the positivity for these schemes is done via M-matrices arguments.

Our next contribution is to propose for the first time a combination of these gradient flow schemes with dimensional splitting technique allowing for fully discrete implicit finite volume schemes for equation (1.1) that are both positivity-preserving and energy-decaying in higher dimensions with a reasonable computational cost. Let us remark that a direct generalisation of the one dimensional scheme presented here and in [1] to higher dimension is possible but comes at a very high dimensional cost resulting from the inversion of large Jacobian matrices. Our scheme takes advantage of the dimensional splitting to drastically reduce this cost without sacrificing the main properties.

Section 2 will discuss the time discretisation for (1.1) in a way that preserves the energy dissipation for general nonlinearities and interaction potentials. Section 3 is devoted to the fully discrete scheme in the one dimensional setting while Section 4 shows the formulation properties for the splitting scheme in two dimensions. Section 5 is aimed at validating the numerical scheme on explicit solutions for both nonlinear diffusions and aggregations. Finally, Section 6 presents numerical experiments that showcase the effectiveness of the new scheme in dealing with complicated phenomena such as metastability and phase transitions, both in one and two dimensions, with linear and nonlinear diffusions.

## 2 Time Discretisation

The choice of time discretisation is critical when trying to construct a fully discrete energy-decaying scheme. In this section we consider two discretisations which will lead to two fully discrete schemes, discussed in the next section.

To begin, we define the semi-discrete energy at time  $t^n$  as follows:

$$E(\rho^n) = \int_{\mathbb{R}^d} H(\rho^n) + V\rho^n + \frac{1}{2}(W * \rho^n)\rho^n \, d\mathbf{x}.$$

For the sake of generality, consider the following first order scheme:

$$\frac{\rho^{n+1} - \rho^n}{\Delta t} = \nabla \cdot (\rho^* \nabla (H'(\rho^{n+1}) + V + W * \rho^{**})), \quad (2.1)$$

where  $\rho^*$  and  $\rho^{**}$  can be either  $\rho^n$  or  $\rho^{n+1}$  and will be specified later. We aim to show that the scheme (2.1) verifies  $E(\rho^{n+1}) \leq E(\rho^n)$ , provided  $\rho^n \geq 0$  at any time step  $t^n$ . To this end, let us first multiply both sides of (2.1) by  $H'(\rho^{n+1}) + V + W * \rho^{**}$  and integrate to obtain

$$\int_{\mathbb{R}^d} (\rho^{n+1} - \rho^n)(H'(\rho^{n+1}) + V + W * \rho^{**}) \, d\mathbf{x} = -\Delta t \int_{\mathbb{R}^d} \rho^* |\nabla (H'(\rho^{n+1}) + V + W * \rho^{**})|^2 \, d\mathbf{x}, \quad (2.2)$$

where the integration by parts was applied on the right hand side. From (2.2), we have

$$\int_{\mathbb{R}^d} (\rho^{n+1} - \rho^n)V \, d\mathbf{x} = - \int_{\mathbb{R}^d} (\rho^{n+1} - \rho^n)(H'(\rho^{n+1}) + W * \rho^{**}) \, d\mathbf{x}$$

$$-\Delta t \int_{\mathbb{R}^d} \rho^* |\nabla(H'(\rho^{n+1}) + V + W * \rho^{**})|^2 \, d\mathbf{x}. \quad (2.3)$$

Then

$$\begin{aligned} E(\rho^{n+1}) - E(\rho^n) &= \int_{\mathbb{R}^d} H(\rho^{n+1}) - H(\rho^n) + (\rho^{n+1} - \rho^n)V + \frac{1}{2}(W * \rho^{n+1})\rho^{n+1} - \frac{1}{2}(W * \rho^n)\rho^n \, d\mathbf{x} \\ &= \int_{\mathbb{R}^d} H(\rho^{n+1}) - H(\rho^n) - (\rho^{n+1} - \rho^n)H'(\rho^{n+1}) \, d\mathbf{x} \\ &\quad + \int_{\mathbb{R}^d} \frac{1}{2}(W * \rho^{n+1})\rho^{n+1} - \frac{1}{2}(W * \rho^n)\rho^n - (\rho^{n+1} - \rho^n)(W * \rho^{**}) \, d\mathbf{x} \\ &\quad - \Delta t \int_{\mathbb{R}^d} \rho^* |\nabla(H'(\rho^{n+1}) + V + W * \rho^{**})|^2 \, d\mathbf{x} \\ &= I + II + III, \end{aligned}$$

where we used (2.3) in the second equality, and

$$\begin{aligned} I &:= \int_{\mathbb{R}^d} H(\rho^{n+1}) - H(\rho^n) - (\rho^{n+1} - \rho^n)H'(\rho^{n+1}) \, d\mathbf{x}; \\ II &:= \int_{\mathbb{R}^d} \frac{1}{2}(W * \rho^{n+1})\rho^{n+1} - \frac{1}{2}(W * \rho^n)\rho^n - (\rho^{n+1} - \rho^n)(W * \rho^{**}) \, d\mathbf{x}; \\ III &:= -\Delta t \int_{\mathbb{R}^d} \rho^* |\nabla(H'(\rho^{n+1}) + V + W * \rho^{**})|^2 \, d\mathbf{x}. \end{aligned}$$

Our goal is to show that  $I + II + III \leq 0$ , hence  $E(\rho^{n+1}) \leq E(\rho^n)$ . In part  $I$

$$H(\rho^{n+1}) - H(\rho^n) \leq (\rho^{n+1} - \rho^n)H'(\rho^{n+1}),$$

which follows from the convexity of  $H$ ; hence  $I \leq 0$  as already pointed out in [3, 29].

In part  $II$  there are several possible choices for  $\rho^{**}$ :

- If  $\rho^{**} = \rho^n$ , we have

$$\begin{aligned} II(\rho^n) &:= \int_{\mathbb{R}^d} \frac{1}{2}(W * \rho^{n+1})\rho^{n+1} - \frac{1}{2}(W * \rho^n)\rho^n - (\rho^{n+1} - \rho^n)(W * \rho^n) \, d\mathbf{x} \\ &= \frac{1}{2} \int_{\mathbb{R}^d} [(W * \rho^{n+1})\rho^{n+1} - 2(W * \rho^n)\rho^{n+1} + (W * \rho^n)\rho^n] \, d\mathbf{x} \\ &= \frac{1}{2} \iint_{\mathbb{R}^{2d}} W(\mathbf{x} - \mathbf{y})(\rho^{n+1}(\mathbf{x}) - \rho^n(\mathbf{x}))(\rho^{n+1}(\mathbf{y}) - \rho^n(\mathbf{y})) \, d\mathbf{x} \, d\mathbf{y}, \end{aligned}$$

since  $W$  is symmetric. We consider two kinds of interaction potentials  $W$ :

- if  $W(\mathbf{x}) = \frac{|\mathbf{x}|^2}{2}$ :

$$\begin{aligned} II(\rho^n) &= \frac{1}{2} \iint_{\mathbb{R}^{2d}} \left( \frac{|\mathbf{x}|^2}{2} - \mathbf{x} \cdot \mathbf{y} + \frac{|\mathbf{y}|^2}{2} \right) (\rho^{n+1}(\mathbf{x}) - \rho^n(\mathbf{x}))(\rho^{n+1}(\mathbf{y}) - \rho^n(\mathbf{y})) \, d\mathbf{x} \, d\mathbf{y} \\ &= \frac{1}{2} \left[ \left( \int_{\mathbb{R}^d} \frac{|\mathbf{x}|^2}{2} (\rho^{n+1}(\mathbf{x}) - \rho^n(\mathbf{x})) \, d\mathbf{x} \right) \left( \int_{\mathbb{R}^d} \rho^{n+1}(\mathbf{y}) - \rho^n(\mathbf{y}) \, d\mathbf{y} \right) \right. \\ &\quad + \left( \int_{\mathbb{R}^d} \frac{|\mathbf{y}|^2}{2} (\rho^{n+1}(\mathbf{y}) - \rho^n(\mathbf{y})) \, d\mathbf{y} \right) \left( \int_{\mathbb{R}^d} \rho^{n+1}(\mathbf{x}) - \rho^n(\mathbf{x}) \, d\mathbf{x} \right) \\ &\quad \left. - \left( \int_{\mathbb{R}^d} \mathbf{x}(\rho^{n+1}(\mathbf{x}) - \rho^n(\mathbf{x})) \, d\mathbf{x} \right) \cdot \left( \int_{\mathbb{R}^d} \mathbf{y}(\rho^{n+1}(\mathbf{y}) - \rho^n(\mathbf{y})) \, d\mathbf{y} \right) \right] \\ &= -\frac{1}{2} \left| \int_{\mathbb{R}^d} \mathbf{x}(\rho^{n+1}(\mathbf{x}) - \rho^n(\mathbf{x})) \, d\mathbf{x} \right|^2 \leq 0, \end{aligned}$$

where we used the fact that  $\int_{\mathbb{R}^d} \rho^{n+1}(\mathbf{x}) \, d\mathbf{x} = \int_{\mathbb{R}^d} \rho^n(\mathbf{x}) \, d\mathbf{x}$ ;

– if  $\hat{W}(\xi) \leq 0$ , where  $\hat{W}(\xi)$  is the Fourier transform of  $W(\mathbf{x})$ :

$$\begin{aligned}
II(\rho^n) &= \frac{1}{2} \int_{\mathbb{R}^d} (W * (\rho^{n+1} - \rho^n))(\mathbf{x})(\rho^{n+1}(\mathbf{x}) - \rho^n(\mathbf{x})) \, d\mathbf{x} \\
&= \frac{1}{2} \iint_{\mathbb{R}^{2d}} \hat{W}(\xi)(\hat{\rho}^{n+1}(\xi) - \hat{\rho}^n(\xi))(\rho^{n+1}(\mathbf{x}) - \rho^n(\mathbf{x}))e^{2\pi i \mathbf{x} \cdot \xi} \, d\xi \, d\mathbf{x} \\
&= \frac{1}{2} \int_{\mathbb{R}^d} \hat{W}(\xi)(\hat{\rho}^{n+1}(\xi) - \hat{\rho}^n(\xi))(\hat{\rho}^{n+1}(-\xi) - \hat{\rho}^n(-\xi)) \, d\xi \\
&= \frac{1}{2} \int_{\mathbb{R}^d} \hat{W}(\xi)(\hat{\rho}^{n+1}(\xi) - \hat{\rho}^n(\xi))(\overline{\hat{\rho}^{n+1}(\xi)} - \overline{\hat{\rho}^n(\xi)}) \, d\xi \\
&= \frac{1}{2} \int_{\mathbb{R}^d} \hat{W}(\xi)|\hat{\rho}^{n+1}(\xi) - \hat{\rho}^n(\xi)|^2 \, d\xi \leq 0.
\end{aligned}$$

• If  $\rho^{**} = \rho^{n+1}$ , we have

$$\begin{aligned}
II(\rho^{n+1}) &:= \int_{\mathbb{R}^d} \frac{1}{2} (W * \rho^{n+1})\rho^{n+1} - \frac{1}{2} (W * \rho^n)\rho^n - (\rho^{n+1} - \rho^n)(W * \rho^{n+1}) \, d\mathbf{x} \\
&= -\frac{1}{2} \int_{\mathbb{R}^d} [(W * \rho^{n+1})\rho^{n+1} - 2(W * \rho^n)\rho^{n+1} + (W * \rho^n)\rho^n] \, d\mathbf{x} \\
&= -\frac{1}{2} \iint_{\mathbb{R}^{2d}} W(\mathbf{x} - \mathbf{y})(\rho^{n+1}(\mathbf{x}) - \rho^n(\mathbf{x}))(\rho^{n+1}(\mathbf{y}) - \rho^n(\mathbf{y})) \, d\mathbf{x} \, d\mathbf{y} = -II(\rho^n),
\end{aligned}$$

which is just the opposite of the previous case. Thus we conclude that for  $W(\mathbf{x}) = -\frac{|\mathbf{x}|^2}{2}$  and  $\hat{W}(\xi) \geq 0$ ,  $II(\rho^{n+1}) \leq 0$ .

• If  $\rho^{**} = \frac{\rho^{n+1} + \rho^n}{2}$ , we have

$$II = \int_{\mathbb{R}^d} \frac{1}{2} (W * \rho^{n+1})\rho^{n+1} - \frac{1}{2} (W * \rho^n)\rho^n - \frac{1}{2} (\rho^{n+1} - \rho^n)(W * (\rho^{n+1} + \rho^n)) \, d\mathbf{x} = 0.$$

Therefore  $II$  is precisely zero regardless of the choice of  $W$ .

Finally,  $III \leq 0$  is clear following from the positivity of either  $\rho^* = \rho^n$  or  $\rho^{n+1}$ .

Let us remark that the above computations remain unchanged when considered over a bounded domain  $\Omega$  with no-flux boundary conditions. It is a simple exercise to check that the boundary terms left by the integration by parts vanish.

Henceforth an interaction  $W$  satisfying  $II(\rho^n) = -II(\rho^{n+1}) \leq 0$  (resp.  $II(\rho^n) = -II(\rho^{n+1}) \geq 0$ ) will be referred as a negative (resp. positive) interaction potential. We have just shown above that attractive (resp. repulsive) quadratic potentials and certain catastrophic (resp. H-stable) potentials, according to the classical statistical mechanics notation in [51], are negative (resp. positive). These potentials are very relevant in applications, both for the existence of steady states and of phase transitions with and without the linear or nonlinear diffusion terms; see [17, 24, 25, 37, 5, 30] and the references therein.

To summarise, a good choice of  $\rho^{**}$  given  $W$  always exists, and we have obtained two time discretisation methods which satisfy an energy dissipation property:

**Proposition 2.1.** *The implicit time discretisation*

$$\frac{\rho^{n+1} - \rho^n}{\Delta t} = \nabla \cdot (\rho^n \nabla (H'(\rho^{n+1}) + V + W * \rho^{**})), \tag{2.4}$$

is energy decaying, i.e.,  $E(\rho^{n+1}) \leq E(\rho^n)$ , if one of the following conditions holds: i)  $\rho^{**} = \frac{\rho^{n+1} + \rho^n}{2}$ ; ii)  $\rho^{**} = \rho^n$  and  $W$  is a negative interaction potential; iii)  $\rho^{**} = \rho^{n+1}$  and  $W$  is a positive interaction potential.

The implicit time discretisation

$$\frac{\rho^{n+1} - \rho^n}{\Delta t} = \nabla \cdot (\rho^{n+1} \nabla (H'(\rho^{n+1}) + V + W * \rho^{**})), \quad (2.5)$$

is energy decaying, i.e.,  $E(\rho^{n+1}) \leq E(\rho^n)$ , if one of the following conditions holds: i)  $\rho^{**} = \frac{\rho^{n+1} + \rho^n}{2}$ ; ii)  $\rho^{**} = \rho^n$  and  $W$  is a negative interaction potential; iii)  $\rho^{**} = \rho^{n+1}$  and  $W$  is a positive interaction potentials.

It is an interesting open problem to show that the schemes (2.4) and (2.5) are well posed in the set of nonnegative densities for small enough  $\Delta t$  under reasonable assumptions on the potentials.

### 3 Fully Discrete Schemes in 1D

In this section we present fully discrete schemes in 1D by coupling the previously introduced time discretisation with the finite volume method in space. We introduce two schemes corresponding to the two time discretisations in (2.4) and (2.5). To begin we consider a large computational domain  $[-L, L]$  and divide it into  $2M$  uniform cells with size  $\Delta x = L/M$ , denoting the  $i$ -th cell ( $i = 1, \dots, 2M$ ) by  $I_i = [x_{i-1/2}, x_{i+1/2}]$ ;  $x_i = -L + \frac{\Delta x}{2} + \Delta x(i-1)$  is the cell center. No-flux boundary conditions are assumed at the boundaries.

#### 3.1 Scheme 1 (S1)

This scheme is based on the implicit time discretisation (2.4). The spatial discretisation follows the fully explicit finite volume method in [20], where only semi-discrete (continuous in time) energy decay was shown. By modifying certain terms into implicit form we obtain a fully discrete energy-decaying scheme with second order accuracy in space.

Assume  $\rho_i$  is the cell average on  $I_i$ ; the scheme thus reads

$$\frac{\rho_i^{n+1} - \rho_i^n}{\Delta t} + \frac{F_{i+1/2}^{n+1} - F_{i-1/2}^{n+1}}{\Delta x} = 0, \quad (3.1a)$$

$$F_{i+1/2}^{n+1} = \rho_i^E (u_{i+1/2}^{n+1})^+ + \rho_{i+1}^W (u_{i+1/2}^{n+1})^-, \quad (3.1b)$$

$$(u_{i+1/2}^{n+1})^+ = \max(u_{i+1/2}^{n+1}, 0), \quad (u_{i+1/2}^{n+1})^- = \min(u_{i+1/2}^{n+1}, 0), \quad (3.1c)$$

$$u_{i+1/2}^{n+1} = -\frac{\xi_{i+1}^{n+1} - \xi_i^{n+1}}{\Delta x}, \quad (3.1d)$$

$$\xi_i^{n+1} = H'(\rho_i^{n+1}) + V_i + (W * \rho^{**})_i, \quad (3.1e)$$

$$\rho_i^E = \rho_i^n + \frac{\Delta x}{2} (\rho_x)_i^n, \quad \rho_i^W = \rho_i^n - \frac{\Delta x}{2} (\rho_x)_i^n, \quad (3.1f)$$

$$(\rho_x)_i^n = \text{minmod} \left( \theta \frac{\rho_{i+1}^n - \rho_i^n}{\Delta x}, \frac{\rho_{i+1}^n - \rho_{i-1}^n}{2\Delta x}, \theta \frac{\rho_i^n - \rho_{i-1}^n}{\Delta x} \right). \quad (3.1g)$$

As suggested previously  $\rho^{**}$  could be  $\rho^n$ ,  $\rho^{n+1}$ , or  $\frac{\rho^n + \rho^{n+1}}{2}$ .  $V_i = V(x_i)$ ,  $(W * \rho^{**})_i = \sum_{j=1}^{2M} W_{i-j} \rho_j^{**} \Delta x$ , where  $W_{i-j} = W(x_i - x_j)$ . The minmod limiter is defined as

$$\text{minmod}(z_1, z_2, \dots) := \begin{cases} \min(z_1, z_2, \dots), & \text{if all } z_i > 0, \\ \max(z_1, z_2, \dots), & \text{if all } z_i < 0, \\ 0, & \text{otherwise,} \end{cases} \quad (3.2)$$

and we choose  $\theta = 2$ .

**Remark 3.1.** One might be interested in potentials  $W$  with an integrable singularity at the origin, as is the case in [20]. In that situation the definition of  $W_{i-j}$  is modified to an integral form

$$W_{i-j} = \frac{1}{\Delta x} \int_{I_j} W(x_i - s) ds \quad (3.3)$$

along the corresponding cell.

### 3.1.1 Positivity

**Theorem 3.1.** *The scheme (3.1) is positivity-preserving; if  $\rho_i^n \geq 0$  for all  $i$ , then  $\rho_i^{n+1} \geq 0$  for all  $i$ , provided the following sufficient CFL condition is satisfied:*

$$\Delta t \leq \frac{\Delta x}{2 \max_i \left\{ (u_{i+1/2}^{n+1})^+, -(u_{i+1/2}^{n+1})^- \right\}}. \quad (3.4)$$

*Proof.* From the definition of the scheme in (3.1), we have

$$\frac{\rho_i^{n+1} - \rho_i^n}{\Delta t} + \frac{\rho_i^E (u_{i+1/2}^{n+1})^+ + \rho_{i+1}^W (u_{i+1/2}^{n+1})^- - \rho_{i-1}^E (u_{i-1/2}^{n+1})^+ - \rho_i^W (u_{i-1/2}^{n+1})^-}{\Delta x} = 0, \quad (3.5)$$

hence

$$\begin{aligned} \rho_i^{n+1} &= \frac{1}{2} (\rho_i^E + \rho_i^W) - \frac{\Delta t}{\Delta x} \left( \rho_i^E (u_{i+1/2}^{n+1})^+ + \rho_{i+1}^W (u_{i+1/2}^{n+1})^- - \rho_{i-1}^E (u_{i-1/2}^{n+1})^+ - \rho_i^W (u_{i-1/2}^{n+1})^- \right) \\ &= \frac{\Delta t}{\Delta x} (u_{i-1/2}^{n+1})^+ \rho_{i-1}^E + \left( \frac{1}{2} - \frac{\Delta t}{\Delta x} (u_{i+1/2}^{n+1})^+ \right) \rho_i^E + \left( \frac{1}{2} + \frac{\Delta t}{\Delta x} (u_{i-1/2}^{n+1})^- \right) \rho_i^W - \frac{\Delta t}{\Delta x} (u_{i+1/2}^{n+1})^- \rho_{i+1}^W. \end{aligned}$$

By the construction, if  $\rho_i^n \geq 0$ , then  $\rho_i^E, \rho_i^W \geq 0$ . Moreover,  $(u_{i-1/2}^{n+1})^+ \geq 0$ ,  $(u_{i+1/2}^{n+1})^- \leq 0$ . Provided the CFL condition (3.4) is satisfied,  $\rho_i^{n+1}$  is a sum of nonnegative values, hence  $\rho_i^{n+1} \geq 0$ .  $\square$

**Remark 3.2.** For the first order scheme,  $\rho_i^E = \rho_i^W = \rho_i^n$ , (3.5) becomes

$$\frac{\rho_i^{n+1} - \rho_i^n}{\Delta t} + \frac{\rho_i^n (u_{i+1/2}^{n+1})^+ + \rho_{i+1}^n (u_{i+1/2}^{n+1})^- - \rho_{i-1}^n (u_{i-1/2}^{n+1})^+ - \rho_i^n (u_{i-1/2}^{n+1})^-}{\Delta x} = 0,$$

i.e.,

$$\rho_i^{n+1} = \left( 1 - \frac{\Delta t}{\Delta x} (u_{i+1/2}^{n+1})^+ + \frac{\Delta t}{\Delta x} (u_{i-1/2}^{n+1})^- \right) \rho_i^n + \frac{\Delta t}{\Delta x} \rho_{i-1}^n (u_{i-1/2}^{n+1})^+ - \frac{\Delta t}{\Delta x} \rho_{i+1}^n (u_{i+1/2}^{n+1})^-.$$

Hence a sufficient CFL condition to guarantee positivity can be

$$\Delta t \leq \frac{\Delta x}{\max_i \left\{ (u_{i+1/2}^{n+1})^+, -(u_{i-1/2}^{n+1})^- \right\}}.$$

**Remark 3.3.** Since  $u_{i+1/2}^{n+1} = \mathcal{O}(\Delta x^{-1})$ , a parabolic type CFL condition  $\Delta t = \mathcal{O}(\Delta x^2)$  is normally required for both first and second order schemes to be positivity-preserving.

### 3.1.2 Energy Decay

We define the fully discrete free energy at time  $t^n$  as follows:

$$E_\Delta(\rho^n) = \Delta x \left( \sum_{i=1}^{2M} H(\rho_i^n) + \sum_{i=1}^{2M} V_i \rho_i^n + \frac{\Delta x}{2} \sum_{i,j=1}^{2M} W_{i-j} \rho_i^n \rho_j^n \right). \quad (3.6)$$

We would like to show  $E_\Delta(\rho^n)$  decays at each time step. For that it is useful to introduce a classification for interaction potentials, following the discussion in Section 2:

**Definition 3.1.** Assume  $\rho_i^n \geq 0$  in the interval  $[-L, L]$  and zero outside of it at any time step  $n$ . A potential  $W$  such that  $\sum_{i,j=1}^{2M} W_{i-j}(\rho_i^{n+1} - \rho_i^n)(\rho_j^{n+1} - \rho_j^n) \leq 0$  (resp.  $\sum_{i,j=1}^{2M} W_{i-j}(\rho_i^{n+1} - \rho_i^n)(\rho_j^{n+1} - \rho_j^n) \geq 0$ ) is called a negative (resp. positive) interaction potential.

We can identify the following potentials as being negative (resp. positive):

**Proposition 3.1.** A quadratic potential  $W(x) = \frac{x^2}{2}$  (resp.  $W(x) = -\frac{x^2}{2}$ ) and a potential such that  $\hat{W}_k \leq 0$  (resp.  $\hat{W}_k \geq 0$ ) for all  $k = 1, \dots, 4M$ , where  $\hat{W}_k = \sum_{i=-M+1}^{3M} W_i \exp^{-2\pi i \frac{(i+M-1)(k-1)}{4M}}$  is the discrete Fourier transform of the sequence  $W_i = W(x_i)$  defined on  $[-2L, 2L]$ , are negative (resp. positive).

*Proof.* If  $W(x) = \frac{x^2}{2}$ , then

$$\begin{aligned} \sum_{i,j=1}^{2M} W_{i-j}(\rho_i^{n+1} - \rho_i^n)(\rho_j^{n+1} - \rho_j^n) &= \sum_{i,j=1}^{2M} \frac{(x_i - x_j)^2}{2} (\rho_i^{n+1} - \rho_i^n)(\rho_j^{n+1} - \rho_j^n) \\ &= \sum_{i=1}^{2M} x_i^2 (\rho_i^{n+1} - \rho_i^n) \sum_{j=1}^{2M} (\rho_j^{n+1} - \rho_j^n) - \left( \sum_{i=1}^{2M} x_i (\rho_i^{n+1} - \rho_i^n) \right)^2 \\ &= - \left( \sum_{i=1}^{2M} x_i (\rho_i^{n+1} - \rho_i^n) \right)^2 \leq 0, \end{aligned}$$

where we used the fact that the scheme (3.1) is conservative,  $\sum_{i=1}^{2M} \rho_i^n = \sum_{i=1}^{2M} \rho_i^{n+1}$ , under the no-flux boundary condition.

If  $W(x)$  is such that  $\hat{W}_k \leq 0$  for all  $k = 1, \dots, 4M$ , then

$$\begin{aligned} \sum_{i,j=1}^{2M} W_{i-j}(\rho_i^{n+1} - \rho_i^n)(\rho_j^{n+1} - \rho_j^n) &= \sum_{i=-M+1}^{3M} \sum_{j=-M+1}^{3M} W_{i-j}(\rho_i^{n+1} - \rho_i^n)(\rho_j^{n+1} - \rho_j^n) \\ &= \frac{1}{4M} \sum_{i=-M+1}^{3M} \sum_{k=1}^{4M} \hat{W}_k (\hat{\rho}_k^{n+1} - \hat{\rho}_k^n) \exp^{2\pi i \frac{(i+M-1)(k-1)}{4M}} (\rho_i^{n+1} - \rho_i^n) \\ &= \frac{1}{4M} \sum_{k=1}^{4M} \hat{W}_k (\hat{\rho}_k^{n+1} - \hat{\rho}_k^n) \overline{(\hat{\rho}_k^{n+1} - \hat{\rho}_k^n)} \\ &= \frac{1}{4M} \sum_{k=1}^{4M} \hat{W}_k |\hat{\rho}_k^{n+1} - \hat{\rho}_k^n|^2 \leq 0, \end{aligned}$$

where the first equality extends summation to the interval  $[-2L, 2L]$  since  $\rho_i^n = 0$  outside  $[-L, L]$ , and the second equality uses the discrete circular convolution theorem and assumes that the sequence  $W_i$  defined on  $[-2L, 2L]$  is periodically extended to the whole space  $\mathbb{R}$ .  $\square$

We can now state the following:

**Theorem 3.2.** Under the CFL condition (3.4), the scheme (3.1) satisfies an energy-decay property, i.e.,  $E_\Delta(\rho^{n+1}) \leq E_\Delta(\rho^n)$ , if one of the following condition holds: (i)  $\rho^{**} = \frac{\rho^n + \rho^{n+1}}{2}$ ; (ii)  $\rho^{**} = \rho^n$  and the potential  $W$  is negative; (iii)  $\rho^{**} = \rho^{n+1}$  and the potential  $W$  is positive.

*Proof.* From the scheme (3.1) it follows

$$\sum_{i=1}^{2M} (\rho_i^{n+1} - \rho_i^n) \xi_i^{n+1} = -\frac{\Delta t}{\Delta x} \sum_{i=1}^{2M} (F_{i+1/2}^{n+1} - F_{i-1/2}^{n+1}) \xi_i^{n+1},$$

with  $\xi_i^{n+1} = H'(\rho_i^{n+1}) + V_i + \sum_{j=1}^{2M} W_{i-j} \rho_j^{**} \Delta x$ . We can rewrite it as in (2.3) to obtain

$$\sum_{i=1}^{2M} (\rho_i^{n+1} - \rho_i^n) V_i = -\frac{\Delta t}{\Delta x} \sum_{i=1}^{2M} (F_{i+1/2}^{n+1} - F_{i-1/2}^{n+1}) \xi_i^{n+1} - \sum_{i=1}^{2M} (\rho_i^{n+1} - \rho_i^n) \left( H'(\rho_i^{n+1}) + \sum_{j=1}^{2M} W_{i-j} \rho_j^{**} \Delta x \right).$$

Using the definition of (3.6) and the identity above, we deduce

$$\begin{aligned} E_\Delta(\rho^{n+1}) - E_\Delta(\rho^n) &= \Delta x \left( \sum_{i=1}^{2M} H(\rho_i^{n+1}) + \sum_{i=1}^{2M} V_i \rho_i^{n+1} + \frac{\Delta x}{2} \sum_{i,j=1}^{2M} W_{i-j} \rho_i^{n+1} \rho_j^{n+1} \right) \\ &\quad - \Delta x \left( \sum_{i=1}^{2M} H(\rho_i^n) + \sum_{i=1}^{2M} V_i \rho_i^n + \frac{\Delta x}{2} \sum_{i,j=1}^{2M} W_{i-j} \rho_i^n \rho_j^n \right) \\ &= \Delta x \sum_{i=1}^{2M} (H(\rho_i^{n+1}) - H(\rho_i^n) - H'(\rho_i^{n+1})(\rho_i^{n+1} - \rho_i^n)) \\ &\quad + \frac{\Delta x^2}{2} \sum_{i,j=1}^{2M} W_{i-j} (\rho_i^{n+1} \rho_j^{n+1} - \rho_i^n \rho_j^n - 2(\rho_i^{n+1} - \rho_i^n) \rho_j^{**}) \\ &\quad - \Delta t \sum_{i=1}^{2M} (F_{i+1/2}^{n+1} - F_{i-1/2}^{n+1}) \xi_i^{n+1} \\ &= I + II + III, \end{aligned}$$

where

$$\begin{aligned} I &:= \Delta x \sum_{i=1}^{2M} (H(\rho_i^{n+1}) - H(\rho_i^n) - H'(\rho_i^{n+1})(\rho_i^{n+1} - \rho_i^n)); \\ II &:= \frac{\Delta x^2}{2} \sum_{i,j=1}^{2M} W_{i-j} (\rho_i^{n+1} \rho_j^{n+1} - \rho_i^n \rho_j^n - 2(\rho_i^{n+1} - \rho_i^n) \rho_j^{**}); \\ III &:= -\Delta t \sum_{i=1}^{2M} (F_{i+1/2}^{n+1} - F_{i-1/2}^{n+1}) \xi_i^{n+1}. \end{aligned}$$

$H(\rho_i^{n+1}) - H(\rho_i^n) - H'(\rho_i^{n+1})(\rho_i^{n+1} - \rho_i^n) \leq 0$  since  $H(\rho)$  is convex, hence  $I \leq 0$ . Considering  $II$ :

- If  $\rho^{**} = \rho^n$ ,

$$II = \frac{\Delta x^2}{2} \sum_{i,j=1}^{2M} W_{i-j} (\rho_i^{n+1} - \rho_i^n) (\rho_j^{n+1} - \rho_j^n).$$

Then  $II \leq 0$  if  $W$  is negative.

- If  $\rho^{**} = \rho^{n+1}$ ,

$$II = -\frac{\Delta x^2}{2} \sum_{i,j=1}^{2M} W_{i-j} (\rho_i^{n+1} - \rho_i^n) (\rho_j^{n+1} - \rho_j^n).$$

Then  $II \leq 0$  if  $W$  is positive.

- if  $\rho^{**} = \frac{\rho^n + \rho^{n+1}}{2}$ ,  $II \equiv 0$ .

Therefore, for the above choices of  $\rho^{**}$  and corresponding  $W$ , we find

$$\begin{aligned}
E_\Delta(\rho^{n+1}) - E_\Delta(\rho^n) &\leq -\Delta t \sum_{i=1}^{2M} \xi_i^{n+1} (F_{i+1/2}^{n+1} - F_{i-1/2}^{n+1}) \\
&= -\Delta t \sum_{i=1}^{2M-1} F_{i+1/2}^{n+1} (\xi_i^{n+1} - \xi_{i+1}^{n+1}) \\
&= -\Delta t \Delta x \sum_{i=1}^{2M-1} F_{i+1/2}^{n+1} u_{i+1/2}^{n+1} \\
&= -\Delta t \Delta x \sum_{i=1}^{2M-1} (\rho_i^E (u_{i+1/2}^{n+1})^+ + \rho_{i+1}^W (u_{i+1/2}^{n+1})^-) u_{i+1/2}^{n+1} \\
&\leq -\Delta t \Delta x \sum_{i=1}^{2M-1} \min(\rho_i^E, \rho_{i+1}^W) |u_{i+1/2}^{n+1}|^2 \leq 0,
\end{aligned}$$

where the first equality employs summation by parts as well as the no-flux boundary condition, and the last inequality relies on the positivity of  $\rho_i$ .  $\square$

## 3.2 Scheme 2 (S2)

This scheme is based on the time discretisation (2.5). The spatial discretisation is the same as the first order version of S1. By modifying certain terms into implicit form, we can obtain a fully discrete unconditionally positive and energy-decaying scheme. This scheme is related to the scheme introduced in [1] for the Keller-Segel model with nonlinear chemosensitivity and linear diffusion.

Assume  $\rho_i$  is the cell average on  $I_i$ ; the scheme thus reads

$$\frac{\rho_i^{n+1} - \rho_i^n}{\Delta t} + \frac{F_{i+1/2}^{n+1} - F_{i-1/2}^{n+1}}{\Delta x} = 0, \quad (3.7a)$$

$$F_{i+1/2}^{n+1} = \begin{cases} \rho_i^{n+1} u_{i+1/2}^{n+1} & \text{if } u_{i+1/2}^{n+1} \geq 0 \\ \rho_{i+1}^{n+1} u_{i+1/2}^{n+1} & \text{if } u_{i+1/2}^{n+1} < 0 \end{cases} = \rho_i^{n+1} (u_{i+1/2}^{n+1})^+ + \rho_{i+1}^{n+1} (u_{i+1/2}^{n+1})^-, \quad (3.7b)$$

$$(u_{i+1/2}^{n+1})^+ = \max(u_{i+1/2}^{n+1}, 0), \quad (u_{i+1/2}^{n+1})^- = \min(u_{i+1/2}^{n+1}, 0), \quad (3.7c)$$

$$u_{i+1/2}^{n+1} = -\frac{\xi_{i+1}^{n+1} - \xi_i^{n+1}}{\Delta x}, \quad (3.7d)$$

$$\xi_i^{n+1} = H'(\rho_i^{n+1}) + V_i + (W * \rho^{**})_i. \quad (3.7e)$$

Again  $\rho^{**}$  may be chosen as  $\rho^n$ ,  $\rho^{n+1}$ , or  $\frac{\rho^n + \rho^{n+1}}{2}$  and  $V_i$  and  $(W * \rho^{**})_i$  are defined as above.

### 3.2.1 Positivity

**Theorem 3.3.** *The scheme (3.7) is unconditionally positive, i.e., if  $\rho_i^n \geq 0$  for all  $i$ , then  $\rho_i^{n+1} \geq 0$  for all  $i$ .*

*Proof.* From the definition of the scheme in (3.7) we find

$$\frac{\rho_i^{n+1} - \rho_i^n}{\Delta t} + \frac{\rho_i^{n+1} (u_{i+1/2}^{n+1})^+ + \rho_{i+1}^{n+1} (u_{i+1/2}^{n+1})^- - \rho_{i-1}^{n+1} (u_{i-1/2}^{n+1})^+ - \rho_i^{n+1} (u_{i-1/2}^{n+1})^-}{\Delta x} = 0,$$

i.e.,

$$\left(1 + \frac{\Delta t}{\Delta x} (u_{i+1/2}^{n+1})^+ - \frac{\Delta t}{\Delta x} (u_{i-1/2}^{n+1})^-\right) \rho_i^{n+1} + \frac{\Delta t}{\Delta x} (u_{i+1/2}^{n+1})^- \rho_{i+1}^{n+1} - \frac{\Delta t}{\Delta x} (u_{i-1/2}^{n+1})^+ \rho_{i-1}^{n+1} = \rho_i^n,$$

which may be written as

$$A(\rho^{n+1})\rho^{n+1} = \rho^n.$$

We would like to show the matrix  $A$  is inverse positive, meaning that every entry of  $A^{-1}$  is nonnegative. We recall a sufficient condition: a matrix  $M$  is inverse positive if  $m_{ij} \leq 0$  for  $i \neq j$ ,  $m_{ii} > 0$ , and strictly diagonally dominant ( $m_{ii} > \sum_{i \neq j} |m_{ij}|$ ). The matrix  $A$  defined above does not satisfy the condition, however  $A^T$  always does. Hence every entry of  $(A^T)^{-1}$  is nonnegative, and thus so are those of  $A^{-1}$ . Therefore, if  $\rho_i^n \geq 0$  for all  $i$ , then  $\rho_i^{n+1} \geq 0$  for all  $i$ .  $\square$

### 3.2.2 Energy Decay

**Theorem 3.4.** *The scheme (3.7) satisfies an energy-decay property unconditionally, i.e.,  $E_\Delta(\rho^{n+1}) \leq E_\Delta(\rho^n)$  as defined in (3.6), if one of the following condition holds: (i)  $\rho^{**} = \frac{\rho^n + \rho^{n+1}}{2}$ ; (ii)  $\rho^{**} = \rho^n$  and the potential  $W$  is negative; (iii)  $\rho^{**} = \rho^{n+1}$  and the potential  $W$  is positive.*

*Proof.* The same proof in the previous section carries over here except the last part:

$$\begin{aligned} E_\Delta(\rho^{n+1}) - E_\Delta(\rho^n) &\leq -\Delta t \sum_{i=1}^{2M} \xi_i^{n+1} (F_{i+1/2}^{n+1} - F_{i-1/2}^{n+1}) \\ &= -\Delta t \sum_{i=1}^{2M-1} F_{i+1/2}^{n+1} (\xi_i^{n+1} - \xi_{i+1}^{n+1}) \\ &= -\Delta t \Delta x \sum_{i=1}^{2M-1} F_{i+1/2}^{n+1} u_{i+1/2}^{n+1} \\ &= -\Delta t \Delta x \sum_{i=1}^{2M-1} (\rho_i^{n+1} (u_{i+1/2}^{n+1})^+ + \rho_{i+1}^{n+1} (u_{i+1/2}^{n+1})^-) u_{i+1/2}^{n+1} \\ &\leq -\Delta t \Delta x \sum_{i=1}^{2M-1} \min(\rho_i^{n+1}, \rho_{i+1}^{n+1}) |u_{i+1/2}^{n+1}|^2 \leq 0, \end{aligned}$$

where the positivity of  $\rho_i$  is used in the last inequality.  $\square$

## 4 Fully Discrete Schemes in 2D Using Dimension Splitting

The previously presented two schemes can be directly extended to any number of dimensions. Here, instead, we propose dimensionally split versions of the 1D schemes and show that the positivity preserving and energy decaying properties are carried over.

The advantage of the dimensional splitting is a huge reduction of the computational cost. Indeed the 1D schemes presented above are implicit, nonlinear, and require the Newton-Raphson method (see Section 5 for further details). It is well known that the cost of inverting a general  $N \times N$  matrix is  $\mathcal{O}(N^3)$  via Gauss-Jordan elimination. If the full  $d$ -dimensional schemes were implemented, the Jacobian matrix inverted at each Newton step would be an  $N^d \times N^d$  matrix, resulting in a  $\mathcal{O}(N^{3d})$  cost. On the other hand, the dimensional splitting in  $d$  dimensions involves performing the inversion of an  $N \times N$  Jacobian  $N^{d-1}$  times, which reduces the cost to  $\mathcal{O}(N^{d+2})$ . Note that the dimensional splitting does not reduce the overall cost of the convolutions.

We proceed to describe 2D versions of the schemes in the splitting framework; the extension to 3D can be done in a similar fashion. For simplicity, assume a square domain  $[-L, L]^2$  and partition both  $x$  and  $y$  uniformly using  $2M$  cells per axis. Then  $\Delta x = \Delta y = L/M$  and the  $ij$ -th cell is denoted by  $I_{i,j} = [x_{i-1/2}, x_{i+1/2}] \times [y_{j-1/2}, y_{j+1/2}]$  with  $x_{i,j} = (-L + \frac{\Delta x}{2} + \Delta x(i-1), -L + \frac{\Delta y}{2} + \Delta y(j-1))$  being the cell center. Again no-flux boundary conditions are assumed at the boundaries.

## 4.1 Scheme 1 (S1)

Assume  $\rho_{i,j}$  is the cell average on cell  $I_{i,j}$ ; the scheme thus reads

- Step 1 - Evolution in  $x$ :

$$\frac{\rho_{i,j}^* - \rho_{i,j}^n}{\Delta t} + \frac{F_{i+1/2,j}^* - F_{i-1/2,j}^*}{\Delta x} = 0, \quad (4.1a)$$

$$F_{i+1/2,j}^* = \rho_{i,j}^E (u_{i+1/2,j}^*)^+ + \rho_{i+1,j}^W (u_{i+1/2,j}^*)^-, \quad (4.1b)$$

$$(u_{i+1/2,j}^*)^+ = \max(u_{i+1/2,j}^*, 0), \quad (u_{i+1/2,j}^*)^- = \min(u_{i+1/2,j}^*, 0), \quad (4.1c)$$

$$u_{i+1/2,j}^* = -\frac{\xi_{i+1,j}^* - \xi_{i,j}^*}{\Delta x}, \quad (4.1d)$$

$$\xi_{i,j}^* = H'(\rho_{i,j}^*) + V_{i,j} + (W * \rho^{**})_{i,j}, \quad (4.1e)$$

$$\rho_{i,j}^E = \rho_{i,j}^n + \frac{\Delta x}{2} (\rho_x)_i^n, \quad \rho_{i,j}^W = \rho_{i,j}^n - \frac{\Delta x}{2} (\rho_x)_{i,j}^n, \quad (4.1f)$$

$$(\rho_x)_{i,j}^n = \text{minmod} \left( \theta \frac{\rho_{i+1,j}^n - \rho_{i,j}^n}{\Delta x}, \frac{\rho_{i+1,j}^n - \rho_{i-1,j}^n}{2\Delta x}, \theta \frac{\rho_{i,j}^n - \rho_{i-1,j}^n}{\Delta x} \right). \quad (4.1g)$$

Once again the choice of  $\rho^{**}$  may be  $\rho^n$ ,  $\rho^*$ , or  $\frac{\rho^n + \rho^*}{2}$ .  $V_{i,j} = V(x_{i,j})$  and

$$(W * \rho^{**})_{i,j} = \sum_{k,l=1}^{2M} W_{i-k,j-l} \rho_{k,l}^{**} \Delta x \Delta y,$$

where  $W_{i-k,j-l} = W(x_i - x_k, y_j - y_l)$ . Remark 3.1 similarly applies for singular potentials in 2D.

- Step 2 - Evolution in  $y$ :

$$\frac{\rho_{i,j}^{n+1} - \rho_{i,j}^*}{\Delta t} + \frac{G_{i,j+1/2}^{n+1} - G_{i,j-1/2}^{n+1}}{\Delta y} = 0, \quad (4.2a)$$

$$G_{i,j+1/2}^{n+1} = \rho_{i,j}^N (v_{i,j+1/2}^{n+1})^+ + \rho_{i,j+1}^S (v_{i,j+1/2}^{n+1})^-, \quad (4.2b)$$

$$(v_{i,j+1/2}^{n+1})^+ = \max(v_{i,j+1/2}^{n+1}, 0), \quad (v_{i,j+1/2}^{n+1})^- = \min(v_{i,j+1/2}^{n+1}, 0), \quad (4.2c)$$

$$v_{i,j+1/2}^{n+1} = -\frac{\xi_{i,j+1}^{n+1} - \xi_{i,j}^{n+1}}{\Delta y}, \quad (4.2d)$$

$$\xi_{i,j}^{n+1} = H'(\rho_{i,j}^{n+1}) + V_{i,j} + (W * \rho^{***})_{i,j}, \quad (4.2e)$$

$$\rho_{i,j}^N = \rho_{i,j}^* + \frac{\Delta x}{2} (\rho_y)_{i,j}^*, \quad \rho_{i,j}^S = \rho_{i,j}^* - \frac{\Delta x}{2} (\rho_y)_{i,j}^*, \quad (4.2f)$$

$$(\rho_y)_{i,j}^* = \text{minmod} \left( \theta \frac{\rho_{i,j+1}^* - \rho_{i,j}^*}{\Delta y}, \frac{\rho_{i,j+1}^* - \rho_{i,j-1}^*}{2\Delta y}, \theta \frac{\rho_{i,j}^* - \rho_{i,j-1}^*}{\Delta y} \right). \quad (4.2g)$$

Here  $\rho^{***}$  may be  $\rho^*$ ,  $\rho^{n+1}$ , or  $\frac{\rho^* + \rho^{n+1}}{2}$ . Other quantities such as  $(W * \rho^{***})_{i,j}$  are defined analogously.

### 4.1.1 Positivity

**Theorem 4.1.** *The scheme (4.1)-(4.2) is positivity preserving provided the following CFL condition is satisfied:*

$$\Delta t \leq \frac{1}{2} \min \left\{ \frac{\Delta x}{\max_{i,j} \{ (u_{i+1/2,j}^*)^+, -(u_{i+1/2,j}^*)^- \}}, \frac{\Delta y}{\max_{i,j} \{ (v_{i,j+1/2}^{n+1})^+, -(v_{i,j+1/2}^{n+1})^- \}} \right\}. \quad (4.3)$$

*Proof.* From the first step (4.1) of the scheme follows that

$$\frac{\rho_{i,j}^* - \rho_{i,j}^n}{\Delta t} + \frac{\rho_{i,j}^E(u_{i+1/2,j}^*)^+ + \rho_{i+1,j}^W(u_{i+1/2,j}^*)^- - \rho_{i-1,j}^E(u_{i-1/2,j}^*)^+ - \rho_{i,j}^W(u_{i-1/2,j}^*)^-}{\Delta x} = 0,$$

hence

$$\begin{aligned} \rho_{i,j}^* &= \frac{1}{2} (\rho_{i,j}^E + \rho_{i,j}^W) - \frac{\Delta t}{\Delta x} \left( \rho_{i,j}^E(u_{i+1/2,j}^*)^+ + \rho_{i+1,j}^W(u_{i+1/2,j}^*)^- - \rho_{i-1,j}^E(u_{i-1/2,j}^*)^+ - \rho_{i,j}^W(u_{i-1/2,j}^*)^- \right) \\ &= \frac{\Delta t}{\Delta x} (u_{i-1/2,j}^*)^+ \rho_{i-1,j}^E + \left( \frac{1}{2} - \frac{\Delta t}{\Delta x} (u_{i+1/2,j}^*)^+ \right) \rho_{i,j}^E \\ &\quad + \left( \frac{1}{2} + \frac{\Delta t}{\Delta x} (u_{i-1/2,j}^*)^- \right) \rho_{i,j}^W - \frac{\Delta t}{\Delta x} (u_{i+1/2,j}^*)^- \rho_{i+1,j}^W. \end{aligned}$$

Since  $\rho_{i,j}^*$  are linear combinations of the nonnegative reconstructed point values  $\rho_{i-1,j}^E$ ,  $\rho_{i,j}^E$ ,  $\rho_{i,j}^W$ ,  $\rho_{i+1,j}^W$  and  $(u_{i-1/2,j}^*)^+ \geq 0$ ,  $(u_{i+1/2,j}^*)^- \leq 0$ , we may conclude that  $\rho_{i,j}^* \geq 0$  provided the CFL condition

$$\Delta t \leq \frac{\Delta x}{2 \max_{i,j} \left\{ (u_{i+1/2,j}^*)^+, -(u_{i+1/2,j}^*)^- \right\}} \quad (4.4)$$

is satisfied.

The second step (4.2) follows analogously:

$$\frac{\rho_{i,j}^{n+1} - \rho_{i,j}^*}{\Delta t} + \frac{\rho_{i,j}^N(v_{i,j+1/2}^{n+1})^+ + \rho_{i,j+1}^S(v_{i,j+1/2}^{n+1})^- - \rho_{i,j-1}^N(v_{i,j-1/2}^{n+1})^+ - \rho_{i,j}^S(v_{i,j-1/2}^{n+1})^-}{\Delta y} = 0,$$

hence

$$\begin{aligned} \rho_{i,j}^{n+1} &= \frac{1}{2} (\rho_{i,j}^N + \rho_{i,j}^S) - \frac{\Delta t}{\Delta y} \left( \rho_{i,j}^N(v_{i,j+1/2}^{n+1})^+ + \rho_{i,j+1}^S(v_{i,j+1/2}^{n+1})^- - \rho_{i,j-1}^N(v_{i,j-1/2}^{n+1})^+ - \rho_{i,j}^S(v_{i,j-1/2}^{n+1})^- \right) \\ &= \frac{\Delta t}{\Delta y} (v_{i,j-1/2}^{n+1})^+ \rho_{i,j-1}^N + \left( \frac{1}{2} - \frac{\Delta t}{\Delta y} (v_{i,j+1/2}^{n+1})^+ \right) \rho_{i,j}^N + \left( \frac{1}{2} + \frac{\Delta t}{\Delta y} (v_{i,j-1/2}^{n+1})^- \right) \rho_{i,j}^S - \frac{\Delta t}{\Delta y} (v_{i,j+1/2}^{n+1})^- \rho_{i,j+1}^S. \end{aligned}$$

Once more  $\rho_{i,j}^{n+1}$  are linear combinations of nonnegative reconstructed point values  $\rho_{i,j-1}^N$ ,  $\rho_{i,j}^N$ ,  $\rho_{i,j}^S$ ,  $\rho_{i,j+1}^S$  and  $(v_{i,j-1/2}^{n+1})^+ \geq 0$ ,  $(v_{i,j+1/2}^{n+1})^- \leq 0$ ; positivity,  $\rho_{i,j}^{n+1} \geq 0$ , follows provided the CFL condition

$$\Delta t \leq \frac{\Delta y}{2 \max_{i,j} \left\{ (v_{i,j+1/2}^{n+1})^+, -(v_{i,j+1/2}^{n+1})^- \right\}} \quad (4.5)$$

is satisfied.

The combination of (4.4) and(4.5) yields condition (4.3) in the theorem.  $\square$

### 4.1.2 Energy Decay

We define the fully discrete free energy at time  $t^n$  as follows:

$$E_\Delta(\rho^n) = \Delta x \Delta y \left( \sum_{i,j=1}^{2M} H(\rho_{i,j}^n) + \sum_{i,j=1}^{2M} V_{i,j} \rho_{i,j}^n + \frac{\Delta x \Delta y}{2} \sum_{i,j,k,l=1}^{2M} W_{i-k,j-l} \rho_{i,j}^n \rho_{k,l}^n \right). \quad (4.6)$$

We aim to show  $E_\Delta(\rho^n)$  decays at each time step. Again we introduce the a classification for the interaction potentials:

**Definition 4.1.** Assume  $\overline{\rho_{i,j}}, \widetilde{\rho_{i,j}} \geq 0$  on the domain  $[-L, L]^2$  and zero outside. A potential  $W$  such that  $\sum_{i,j,k,l=1}^{2M} W_{i-k,j-l}(\overline{\rho_{i,j}} - \widetilde{\rho_{i,j}})(\overline{\rho_{k,l}} - \widetilde{\rho_{k,l}}) \leq 0$  (resp.  $\sum_{i,j,k,l=1}^{2M} W_{i-k,j-l}(\overline{\rho_{i,j}} - \widetilde{\rho_{i,j}})(\overline{\rho_{k,l}} - \widetilde{\rho_{k,l}}) \geq 0$ ) is called a negative (resp. positive) interaction potential.

A result similar to Proposition 3.1 can be obtained in 2D to provide the same examples of negative and positive interaction potentials; this we leave to the reader.

**Theorem 4.2.** Under the CFL contion (4.3), the scheme (4.1)-(4.2) satisfies an energy-decay property, i.e.,  $E_{\Delta}(\rho^{n+1}) \leq E_{\Delta}(\rho^n)$  with the definition from (4.6), if one of the following condition holds: (i)  $\rho^{**} = \frac{\rho^n + \rho^{n+1}}{2}$ ; (ii)  $\rho^{**} = \rho^n$  and the potential  $W$  is negative; (iii)  $\rho^{**} = \rho^{n+1}$  and the potential  $W$  is positive.

*Proof.* From step 1 (4.1) follows that

$$\sum_{i,j=1}^{2M} (\rho_{i,j}^* - \rho_{i,j}^n) \xi_{i,j}^* = -\frac{\Delta t}{\Delta x} \sum_{i,j=1}^{2M} (F_{i+1/2,j}^* - F_{i-1/2,j}^*) \xi_{i,j}^*,$$

where  $\xi_{i,j}^* = H'(\rho_{i,j}^*) + V_{i,j} + \sum_{k,l=1}^{2M} W_{i-k,j-l} \rho_{k,l}^{**} \Delta x \Delta y$ ; as in the previous computations in Section 3, we deduce

$$\begin{aligned} E_{\Delta}(\rho^*) - E_{\Delta}(\rho^n) &= \Delta x \Delta y \left( \sum_{i,j=1}^{2M} H(\rho_{i,j}^*) + \sum_{i,j=1}^{2M} V_{i,j} \rho_{i,j}^* + \frac{\Delta x \Delta y}{2} \sum_{i,j,k,l=1}^{2M} W_{i-k,j-l} \rho_{i,j}^* \rho_{k,l}^* \right) \\ &\quad - \Delta x \Delta y \left( \sum_{i,j=1}^{2M} H(\rho_{i,j}^n) + \sum_{i,j=1}^{2M} V_{i,j} \rho_{i,j}^n + \frac{\Delta x \Delta y}{2} \sum_{i,j,k,l=1}^{2M} W_{i-k,j-l} \rho_{i,j}^n \rho_{k,l}^n \right) \\ &= \Delta x \Delta y \sum_{i,j=1}^{2M} (H(\rho_{i,j}^*) - H(\rho_{i,j}^n) - H'(\rho_{i,j}^*)(\rho_{i,j}^* - \rho_{i,j}^n)) \\ &\quad + \frac{(\Delta x \Delta y)^2}{2} \sum_{i,j,k,l=1}^{2M} W_{i-k,j-l} (\rho_{i,j}^* \rho_{k,l}^* - \rho_{i,j}^n \rho_{k,l}^n - 2(\rho_{i,j}^* - \rho_{i,j}^n) \rho_{k,l}^{**}) \\ &\quad - \Delta t \Delta y \sum_{i,j=1}^{2M} (F_{i+1/2,j}^* - F_{i-1/2,j}^*) \xi_{i,j}^*. \end{aligned}$$

The terms involving  $W$  are either  $\leq 0$  or  $\equiv 0$  depending on the choice of  $\rho^{**}$  as in the 1D setting.

From step 2 (4.2) we deduce

$$\sum_{i,j=1}^{2M} (\rho_{i,j}^{n+1} - \rho_{i,j}^*) \xi_{i,j}^{n+1} = -\frac{\Delta t}{\Delta y} \sum_{i,j=1}^{2M} (G_{i,j+1/2}^{n+1} - G_{i,j-1/2}^{n+1}) \xi_{i,j}^{n+1},$$

where  $\xi_{i,j}^{n+1} = H'(\rho_{i,j}^{n+1}) + V_{i,j} + \sum_{k,l=1}^{2M} W_{i-k,j-l} \rho_{k,l}^{***} \Delta x \Delta y$ , and similarly

$$\begin{aligned}
E_{\Delta}(\rho^{n+1}) - E_{\Delta}(\rho^*) &= \Delta x \Delta y \left( \sum_{i,j=1}^{2M} H(\rho_{i,j}^{n+1}) + \sum_{i,j=1}^{2M} V_{i,j} \rho_{i,j}^{n+1} + \frac{\Delta x \Delta y}{2} \sum_{i,j,k,l=1}^{2M} W_{i-k,j-l} \rho_{i,j}^{n+1} \rho_{k,l}^{n+1} \right) \\
&\quad - \Delta x \Delta y \left( \sum_{i,j=1}^{2M} H(\rho_{i,j}^*) + \sum_{i,j=1}^{2M} V_{i,j} \rho_{i,j}^* + \frac{\Delta x \Delta y}{2} \sum_{i,j,k,l=1}^{2M} W_{i-k,j-l} \rho_{i,j}^* \rho_{k,l}^* \right) \\
&= \Delta x \Delta y \sum_{i,j=1}^{2M} (H(\rho_{i,j}^{n+1}) - H(\rho_{i,j}^*) - H'(\rho_{i,j}^{n+1})(\rho_{i,j}^{n+1} - \rho_{i,j}^*)) \\
&\quad + \frac{(\Delta x \Delta y)^2}{2} \sum_{i,j,k,l=1}^{2M} W_{i-k,j-l} (\rho_{i,j}^{n+1} \rho_{k,l}^{n+1} - \rho_{i,j}^* \rho_{k,l}^* - 2(\rho_{i,j}^{n+1} - \rho_{i,j}^*) \rho_{k,l}^{***}) \\
&\quad - \Delta t \Delta x \sum_{i,j=1}^{2M} (G_{i,j+1/2}^{n+1} - G_{i,j-1/2}^{n+1}) \xi_{i,j}^{n+1}.
\end{aligned}$$

Yet again the terms involving  $W$  are either  $\leq 0$  or  $\equiv 0$  depending on the choice of  $\rho^{***}$ , consistently with the first step. Combining the estimates we finally conclude

$$\begin{aligned}
E_{\Delta}(\rho^{n+1}) - E_{\Delta}(\rho^n) &\leq -\Delta t \Delta y \sum_{i,j=1}^{2M} \xi_{i,j}^* (F_{i+1/2,j}^* - F_{i-1/2,j}^*) - \Delta t \Delta x \sum_{i,j=1}^{2M} \xi_{i,j}^{n+1} (G_{i,j+1/2}^{n+1} - G_{i,j-1/2}^{n+1}) \\
&= -\Delta t \Delta y \sum_{i,j=1}^{2M-1} F_{i+1/2,j}^* (\xi_{i,j}^* - \xi_{i+1,j}^*) - \Delta t \Delta x \sum_{i,j=1}^{2M-1} G_{i,j+1/2}^{n+1} (\xi_{i,j}^{n+1} - \xi_{i,j+1}^{n+1}) \\
&= -\Delta t \Delta x \Delta y \sum_{i,j=1}^{2M-1} F_{i+1/2,j}^* u_{i+1/2,j}^* - \Delta t \Delta x \Delta y \sum_{i,j=1}^{2M-1} G_{i,j+1/2}^{n+1} v_{i,j+1/2}^{n+1} \\
&= -\Delta t \Delta x \Delta y \sum_{i,j=1}^{2M-1} (\rho_{i,j}^E (u_{i+1/2,j}^*)^+ + \rho_{i+1,j}^W (u_{i+1/2,j}^*)^-) u_{i+1/2,j}^* \\
&\quad - \Delta t \Delta x \Delta y \sum_{i,j=1}^{2M-1} (\rho_{i,j}^N (v_{i,j+1/2}^{n+1})^+ + \rho_{i,j+1}^S (v_{i,j+1/2}^{n+1})^-) v_{i,j+1/2}^{n+1} \\
&\leq -\Delta t \Delta x \Delta y \sum_{i,j=1}^{2M-1} \min(\rho_{i,j}^E, \rho_{i+1,j}^W) |u_{i+1/2,j}^*|^2 \\
&\quad - \Delta t \Delta x \Delta y \sum_{i,j=1}^{2M-1} \min(\rho_{i,j}^N, \rho_{i,j+1}^S) |v_{i,j+1/2}^{n+1}|^2 \leq 0,
\end{aligned}$$

where we employ the summation by parts, the no-flux boundary condition, and the positivity of  $\rho_{i,j}$ .  $\square$

## 4.2 Scheme 2 (S2)

Assume  $\rho_{i,j}$  is the cell average on cell  $I_{i,j}$ ; the scheme reads

- Step 1 - Evolution in  $x$ :

$$\frac{\rho_{i,j}^* - \rho_{i,j}^n}{\Delta t} + \frac{F_{i+1/2,j}^* - F_{i-1/2,j}^*}{\Delta x} = 0, \tag{4.7a}$$

$$F_{i+1/2,j}^* = \begin{cases} \rho_{i,j}^* u_{i+1/2,j}^* & \text{if } u_{i+1/2,j}^* > 0 \\ \rho_{i+1,j}^* u_{i+1/2,j}^* & \text{if } u_{i+1/2,j}^* < 0 \end{cases} = \rho_{i,j}^* (u_{i+1/2,j}^*)^+ + \rho_{i+1,j}^* (u_{i+1/2,j}^*)^-, \quad (4.7b)$$

$$(u_{i+1/2,j}^*)^+ = \max(u_{i+1/2,j}^*, 0), \quad (u_{i+1/2,j}^*)^- = \min(u_{i+1/2,j}^*, 0), \quad (4.7c)$$

$$u_{i+1/2,j}^* = -\frac{\xi_{i+1,j}^* - \xi_{i,j}^*}{\Delta x}, \quad (4.7d)$$

$$\xi_{i,j}^* = H'(\rho_{i,j}^*) + V_{i,j} + (W * \rho^{**})_{i,j}. \quad (4.7e)$$

Where  $\rho^{**}$  may be  $\rho^n$ ,  $\rho^*$ , or  $\frac{\rho^n + \rho^*}{2}$ .

- Step 2 - Evolution in  $y$ :

$$\frac{\rho_{i,j}^{n+1} - \rho_{i,j}^*}{\Delta t} + \frac{G_{i,j+1/2}^{n+1} - G_{i,j+1/2}^{n+1}}{\Delta y} = 0, \quad (4.8a)$$

$$G_{i,j+1/2}^{n+1} = \begin{cases} \rho_{i,j}^{n+1} v_{i,j+1/2}^{n+1} & \text{if } v_{i,j+1/2}^{n+1} > 0 \\ \rho_{i,j+1}^{n+1} v_{i,j+1/2}^{n+1} & \text{if } v_{i,j+1/2}^{n+1} < 0 \end{cases} = \rho_{i,j}^{n+1} (v_{i,j+1/2}^{n+1})^+ + \rho_{i,j+1}^{n+1} (v_{i,j+1/2}^{n+1})^-, \quad (4.8b)$$

$$(v_{i,j+1/2}^{n+1})^+ = \max(v_{i,j+1/2}^{n+1}, 0), \quad (v_{i,j+1/2}^{n+1})^- = \min(v_{i,j+1/2}^{n+1}, 0), \quad (4.8c)$$

$$v_{i,j+1/2}^{n+1} = -\frac{\xi_{i,j+1}^{n+1} - \xi_{i,j}^{n+1}}{\Delta y}, \quad (4.8d)$$

$$\xi_{i,j}^{n+1} = H'(\rho_{i,j}^{n+1}) + V_{i,j} + (W * \rho^{***})_{i,j}. \quad (4.8e)$$

Where  $\rho^{***}$  can be  $\rho^*$ ,  $\rho^{n+1}$ , or  $\frac{\rho^* + \rho^{n+1}}{2}$ .

#### 4.2.1 Positivity

**Theorem 4.3.** *The scheme (4.7)-(4.8) is unconditionally positive.*

*Proof.* From the first step (4.7) of the scheme follows that

$$\frac{\rho_{i,j}^* - \rho_{i,j}^n}{\Delta t} + \frac{\rho_{i,j}^* (u_{i+1/2,j}^*)^+ + \rho_{i+1,j}^* (u_{i+1/2,j}^*)^- - \rho_{i-1,j}^* (u_{i-1/2,j}^*)^+ - \rho_{i,j}^* (u_{i-1/2,j}^*)^-}{\Delta x} = 0,$$

i.e.,

$$\left(1 + \frac{\Delta t}{\Delta x} (u_{i+1/2,j}^*)^+ - \frac{\Delta t}{\Delta x} (u_{i-1/2,j}^*)^-\right) \rho_{i,j}^* + \frac{\Delta t}{\Delta x} (u_{i+1/2,j}^*)^- \rho_{i+1,j}^* - \frac{\Delta t}{\Delta x} (u_{i-1/2,j}^*)^+ \rho_{i-1,j}^* = \rho_{i,j}^n,$$

which may be written as

$$A(\tilde{\rho}^*) \tilde{\rho}^* = \tilde{\rho}^n, \quad \tilde{\rho}_{(j-1)N+i} = \rho_{i,j},$$

where  $A = (a_{ij})$  is an M-matrix as in the 1D case. Therefore  $\tilde{\rho}_i^* \geq 0$  if  $\tilde{\rho}_i^n \geq 0$  for all  $i$ . Similarly, in the second step (4.8):

$$\frac{\rho_{i,j}^{n+1} - \rho_{i,j}^*}{\Delta t} + \frac{\rho_{i,j}^{n+1} (v_{i,j+1/2}^{n+1})^+ + \rho_{i,j+1}^{n+1} (v_{i,j+1/2}^{n+1})^- - \rho_{i,j-1}^{n+1} (v_{i,j-1/2}^{n+1})^+ - \rho_{i,j}^{n+1} (v_{i,j-1/2}^{n+1})^-}{\Delta y} = 0,$$

i.e.,

$$\left(1 + \frac{\Delta t}{\Delta y} (v_{i,j+1/2}^{n+1})^+ - \frac{\Delta t}{\Delta y} (v_{i,j-1/2}^{n+1})^-\right) \rho_{i,j}^{n+1} + \frac{\Delta t}{\Delta y} (v_{i,j+1/2}^{n+1})^- \rho_{i,j+1}^{n+1} - \frac{\Delta t}{\Delta y} (v_{i,j-1/2}^{n+1})^+ \rho_{i,j-1}^{n+1} = \rho_{i,j}^*,$$

which can be written as

$$A(\tilde{\rho}^{n+1}) \tilde{\rho}^{n+1} = \tilde{\rho}^*, \quad \tilde{\rho}_{(j-1)N+i} = \rho_{i,j},$$

where  $A = (a_{ij})$  is again an M-matrix. Therefore  $\tilde{\rho}_i^{n+1} \geq 0$  if  $\tilde{\rho}_i^* \geq 0$  for all  $i$ .  $\square$

## 4.2.2 Energy Decay

**Theorem 4.4.** *The scheme (4.7)-(4.8) satisfies an energy-decay property unconditionally, i.e.,  $E_\Delta(\rho^{n+1}) \leq E_\Delta(\rho^n)$  with the definition from (4.6), if one of the following condition holds (i)  $\rho^{**} = \frac{\rho^n + \rho^{n+1}}{2}$ ; (ii)  $\rho^{**} = \rho^n$  and the potential  $W$  is negative; (iii)  $\rho^{**} = \rho^{n+1}$  and the potential  $W$  is positive.*

*Proof.* The proof of the result in the previous section carries over except for the last part:

$$\begin{aligned}
E_\Delta(\rho^{n+1}) - E_\Delta(\rho^n) &\leq -\Delta t \Delta y \sum_{i,j=1}^{2M} \xi_{i,j}^* (F_{i+1/2,j}^* - F_{i-1/2,j}^*) - \Delta t \Delta x \sum_{i,j=1}^{2M} \xi_{i,j}^{n+1} (G_{i,j+1/2}^{n+1} - G_{i,j-1/2}^{n+1}) \\
&= -\Delta t \Delta y \sum_{i,j=1}^{2M-1} F_{i+1/2,j}^* (\xi_{i,j}^* - \xi_{i+1,j}^*) - \Delta t \Delta x \sum_{i,j=1}^{2M-1} G_{i,j+1/2}^{n+1} (\xi_{i,j}^{n+1} - \xi_{i,j+1}^{n+1}) \\
&= -\Delta t \Delta x \Delta y \sum_{i,j=1}^{2M-1} F_{i+1/2,j}^* u_{i+1/2,j}^* - \Delta t \Delta x \Delta y \sum_{i,j=1}^{2M-1} G_{i,j+1/2}^{n+1} v_{i,j+1/2}^{n+1} \\
&= -\Delta t \Delta x \Delta y \sum_{i,j=1}^{2M-1} (\rho_{i,j}^* (u_{i+1/2,j}^*)^+ + \rho_{i+1,j}^* (u_{i+1/2,j}^*)^-) u_{i+1/2,j}^* \\
&\quad - \Delta t \Delta x \Delta y \sum_{i,j=1}^{2M-1} (\rho_{i,j}^{n+1} (v_{i,j+1/2}^{n+1})^+ + \rho_{i,j+1}^{n+1} (v_{i,j+1/2}^{n+1})^-) v_{i,j+1/2}^{n+1} \\
&\leq -\Delta t \Delta x \Delta y \sum_{i,j=1}^{2M-1} \min(\rho_{i,j}^*, \rho_{i+1,j}^*) |u_{i+1/2,j}^*|^2 \\
&\quad - \Delta t \Delta x \Delta y \sum_{i,j=1}^{2M-1} \min(\rho_{i,j}^{n+1}, \rho_{i,j+1}^{n+1}) |v_{i,j+1/2}^{n+1}|^2 \leq 0.
\end{aligned}$$

□

## 5 Implementation, Validation and Accuracy of the Schemes

The following section is concerned with the implementation of the numerical schemes as well as their validation against equations whose analytic solution is known. First we validate the order of the schemes by solving the Heat and Porous Medium Equations and studying the error against known analytical solutions. Later on we validate the order of convergence to a stationary state on Nonlinear and Nonlocal analogues of the Fokker-Planck equation by comparing them against known convergence rates. We recall the essential properties of the schemes:

|                            | SCHEME 1 (S1)   | SCHEME 2 (S2) |
|----------------------------|---|---------------|
| Order in time              | First   | First         |
| Order in space             | Second  | First         |
| Positivity-preserving      | $\Delta t \leq \frac{\Delta x}{2 \max_i \{(u_{i+1/2}^{n+1})^+, -(u_{i+1/2}^{n+1})^-\}}$ | Unconditional |
| Full-discrete energy decay |   |               |

### 5.1 Implementation — A Note on Vacuum Solutions

The numerical schemes were implemented using the Julia language [9]. The implicit-in-time formulation of S1 and S2 requires the approximation of the solution  $\rho^{n+1}$  to (3.1) and (3.7), for which we employ

the Newton-Raphson method. Throughout Sections 5 and 6 we make the choice  $\rho^{**} = \frac{\rho^n + \rho^{n+1}}{2}$ , which guarantees the decay of the discrete energy regardless of the choice of  $W$ .

Due to the nature of the schemes, special care should be taken when dealing with problems where vacuum is present. While the schemes perform satisfactorily in cases where segments of the solution take arbitrarily small values (the Heat Equation in Section 5.2, for instance), they sometimes fail with solutions involving zero segments. Examples of this are problems with compactly supported initial data such as the Barenblatt solution for the Porous Medium Equation.

An explicit calculation of the Jacobian matrix of the schemes employed by the Newton solver reveals that certain terms can become ill-posed when  $\rho_i = 0$  in some cells. In particular, terms involving the partial derivative of  $u_{i+1/2}^{n+1}$  with respect to  $\rho_j^{n+1}$  result in the second derivative of the internal energy density,  $H''(\rho)$ , which can be singular. For instance, this is proportional to  $\rho^{m-2}$  for the Heat Equation or the Porous Medium Equation; under S1 the range  $1 \leq m < 2$  is problematic, whereas S2 handles all cases except  $m = 1$ . The issue can be easily circumvented by modifying the energy term to include an offset,  $H(\hat{\rho})$  where  $\hat{\rho} = \max(\rho, \epsilon)$ ; we use  $\epsilon = 10^{-300}$  in the aforementioned cases.

## 5.2 Heat Equation

The first validation case is the Heat Equation  $\rho_t = D\Delta\rho$ , i.e.

$$H(\rho) = D(\rho \log(\rho) - \rho), \quad V(\mathbf{x}) = 0, \quad W(\mathbf{x}) = 0, \quad (5.1)$$

for  $D > 0$ . The analytic solution  $\rho^*(\mathbf{x}, T)$  corresponding to a point source is given by the Heat Kernel

$$\Phi(\mathbf{x}, t) = (4\pi Dt)^{-\frac{n}{2}} \exp\left(-\frac{|\mathbf{x}|^2}{4Dt}\right). \quad (5.2)$$

We will solve (5.1) numerically for  $D = 1$  with initial data  $\rho_0(\mathbf{x}) = \Phi(\mathbf{x}, 0.1)$  through an interval of time of unit length for various choices of  $\Delta x$ . We will compute the  $L_1$  error of the numerical solution  $\rho_{\Delta x}$  at the final time

$$\varepsilon(\Delta x) = \|\rho_{\Delta x}(\mathbf{x}, T) - \rho^*(\mathbf{x}, T)\|_{L_1}.$$

The error will then be used to estimate the order of convergence of the scheme

$$o(\Delta x) = \log_2(\varepsilon(2\Delta x)/\varepsilon(\Delta x)).$$

The choice of  $\Delta t$  is  $\Delta t = \Delta x$  for the S2 validation, but  $\Delta t$  is  $\Delta t = \Delta x^2$  for the S1 validation in order to show second order convergence in space. The results for the S1 scheme can be found on tables 1 and 2 for 1D and 2D respectively. The results for S2 follow on tables 3 and 4. Good approximation to orders 2 and 1 can be seen for S1 and S2 respectively.

| $\Delta x$   | $\varepsilon(\Delta x)$ | $o(\Delta x)$ |
|--------------|-------------------------|---------------|
| 0.5000000000 | 0.2539223807            | —             |
| 0.2500000000 | 0.0703336434            | 1.8521007013  |
| 0.1250000000 | 0.0156514107            | 2.1679222566  |
| 0.0625000000 | 0.0038173870            | 2.0356353397  |
| 0.0312500000 | 0.0009495577            | 2.0072578781  |
| 0.0156250000 | 0.0002370508            | 2.0020594067  |

Table 1: Error table for the solution to the Heat Equation (5.1) with the S1 1D scheme.

| $\Delta x$   | $\varepsilon(\Delta x)$ | $o(\Delta x)$ |
|--------------|-------------------------|---------------|
| 0.5000000000 | 0.4504541128            | —             |
| 0.2500000000 | 0.1182590268            | 1.9294298382  |
| 0.1250000000 | 0.0252129284            | 2.2297147124  |
| 0.0625000000 | 0.0061782321            | 2.0288977169  |
| 0.0312500000 | 0.0015372094            | 2.0068804088  |
| 0.0156250000 | 0.0003838662            | 2.0016381926  |

Table 2: Error table for the solution to the Heat Equation (5.1) with the S1 2D scheme.

| $\Delta x$   | $\varepsilon(\Delta x)$ | $o(\Delta x)$ |
|--------------|-------------------------|---------------|
| 0.5000000000 | 0.1094009564            | —             |
| 0.2500000000 | 0.0568879719            | 0.9434297966  |
| 0.1250000000 | 0.0291692304            | 0.9636763260  |
| 0.0625000000 | 0.0149657164            | 0.9627859813  |
| 0.0312500000 | 0.0076354616            | 0.9708740589  |
| 0.0156250000 | 0.0038695264            | 0.9805583749  |

Table 3: Error table for the solution to the Heat Equation (5.1) with the S2 1D scheme.

| $\Delta x$   | $\varepsilon(\Delta x)$ | $o(\Delta x)$ |
|--------------|-------------------------|---------------|
| 0.5000000000 | 0.1666028380            | —             |
| 0.2500000000 | 0.0903439872            | 0.8829124850  |
| 0.1250000000 | 0.0486209023            | 0.8938519195  |
| 0.0625000000 | 0.0257501601            | 0.9169952648  |
| 0.0312500000 | 0.0133872726            | 0.9437193330  |
| 0.0156250000 | 0.0068538625            | 0.9658729148  |

Table 4: Error table for the solution to the Heat Equation (5.1) with the S2 2D scheme.

### 5.3 Porous Medium Equation

To validate a nonlinear diffusion setting we will next consider the Porous Medium Equation  $\rho_t = D\Delta\rho^m$

$$H(\rho) = \frac{D}{m-1}\rho^m, \quad V(\mathbf{x}) = 0, \quad W(\mathbf{x}) = 0, \quad (5.3)$$

for  $D > 0, m > 1$ . The Barenblatt solution  $\rho^*(\mathbf{x}, T)$  corresponding to a point source is given by

$$\Psi(\mathbf{x}, t) = \frac{1}{t^\alpha} \psi\left(\frac{|\mathbf{x}|}{t^\beta}\right), \quad (5.4)$$

where  $\psi(\xi) = (K - \kappa\xi^2)_+^{1/(m-1)}$  for  $\alpha = n/(n(m-1) + 2)$ ,  $\beta = \alpha/n$ ,  $\gamma = 1/(m-1) + n/2$ ,  $\kappa = \beta(m-1)/(2Dm)$  and  $(\cdot)_+ = \max\{\cdot, 0\}$ . The normalisation constant  $K > 0$  is related to the total mass  $M$  by  $M = a(m, n)K^\gamma$ , see [58, Section 17.5], where

$$a(m, n) = \left(\frac{\pi(2Dmn)}{\alpha(m-1)}\right)^{\frac{n}{2}} \frac{\Gamma\left(\frac{m}{m-1}\right)}{\Gamma\left(\frac{m}{m-1} + \frac{n}{2}\right)}. \quad (5.5)$$

As before, we will solve (5.3) numerically for  $D = 1$  with initial data  $\rho_0(\mathbf{x}) = \Psi(\mathbf{x}, 0.1)$  and estimate the order of the scheme. Tables 5 through 16 correspond to the cases  $m = 3/2$ ,  $m = 2$  and  $m = 3$  for

both schemes in 1D and 2D. The approximation to the correct orders is fine for  $m = 3/2$  but worsens for increasing values of  $m$  when compared to section 5.2. This is well known in the numerical literature for nonlinear diffusion, as the Barenblatt solution and compactly supported solutions in general lose regularity with increasing exponents, see for instance [20].

| $\Delta x$   | $\varepsilon(\Delta x)$ | $o(\Delta x)$ |
|--------------|-------------------------|---------------|
| 0.5000000000 | 0.0204873663            | —             |
| 0.2500000000 | 0.0281822062            | -0.4600500244 |
| 0.1250000000 | 0.0091958216            | 1.6157341810  |
| 0.0625000000 | 0.0022878538            | 2.0069836075  |
| 0.0312500000 | 0.0005414761            | 2.0790252906  |
| 0.0156250000 | 0.0001296092            | 2.0627297631  |

Table 5: Error table for the solution to the Porous Medium Equation (5.3) with  $m = 3/2$  and the S1 1D scheme.

| $\Delta x$   | $\varepsilon(\Delta x)$ | $o(\Delta x)$ |
|--------------|-------------------------|---------------|
| 0.5000000000 | 0.0366134046            | —             |
| 0.2500000000 | 0.0476236527            | -0.3793063443 |
| 0.1250000000 | 0.0149259470            | 1.6738558140  |
| 0.0625000000 | 0.0036819024            | 2.0192991753  |
| 0.0312500000 | 0.0008779327            | 2.0682690586  |
| 0.0156250000 | 0.0002094376            | 2.0675897589  |

Table 6: Error table for the solution to the Porous Medium Equation (5.3) with  $m = 3/2$  and the S1 2D scheme.

| $\Delta x$   | $\varepsilon(\Delta x)$ | $o(\Delta x)$ |
|--------------|-------------------------|---------------|
| 0.5000000000 | 0.1689483411            | —             |
| 0.2500000000 | 0.0919130388            | 0.8782407427  |
| 0.1250000000 | 0.0483686774            | 0.9261964479  |
| 0.0625000000 | 0.0251558610            | 0.9431785200  |
| 0.0312500000 | 0.0129139115            | 0.9619685237  |
| 0.0156250000 | 0.0065738100            | 0.9741243808  |

Table 7: Error table for the solution to the Porous Medium Equation (5.3) with  $m = 3/2$  and the S2 1D scheme.

| $\Delta x$   | $\varepsilon(\Delta x)$ | $o(\Delta x)$ |
|--------------|-------------------------|---------------|
| 0.5000000000 | 0.2579678134            | —             |
| 0.2500000000 | 0.1451886754            | 0.8292621432  |
| 0.1250000000 | 0.0806082194            | 0.8489300706  |
| 0.0625000000 | 0.0429098424            | 0.9096183524  |
| 0.0312500000 | 0.0228310551            | 0.9103110652  |
| 0.0156250000 | 0.0115791626            | 0.9794666096  |

Table 8: Error table for the solution to the Porous Medium Equation (5.3) with  $m = 3/2$  and the S2 2D scheme.

| $\Delta x$   | $\varepsilon(\Delta x)$ | $o(\Delta x)$ |
|--------------|-------------------------|---------------|
| 0.5000000000 | 0.0519736396            | —             |
| 0.2500000000 | 0.0051359775            | 3.3390693083  |
| 0.1250000000 | 0.0017868233            | 1.5232419098  |
| 0.0625000000 | 0.0005409510            | 1.7238270357  |
| 0.0312500000 | 0.0001421120            | 1.9284693896  |
| 0.0156250000 | 0.0000364568            | 1.9627680666  |

Table 9: Error table for the solution to the Porous Medium Equation (5.3) with  $m = 2$  and the S1 1D scheme.

| $\Delta x$   | $\varepsilon(\Delta x)$ | $o(\Delta x)$ |
|--------------|-------------------------|---------------|
| 0.5000000000 | 0.0924621353            | —             |
| 0.2500000000 | 0.0086884832            | 3.4116864351  |
| 0.1250000000 | 0.0028749582            | 1.5955633781  |
| 0.0625000000 | 0.0008814627            | 1.7055695491  |
| 0.0312500000 | 0.0002314568            | 1.9291566094  |
| 0.0156250000 | 0.0000595911            | 1.9575740753  |

Table 10: Error table for the solution to the Porous Medium Equation (5.3) with  $m = 2$  and the S1 2D scheme.

| $\Delta x$   | $\varepsilon(\Delta x)$ | $o(\Delta x)$ |
|--------------|-------------------------|---------------|
| 0.5000000000 | 0.1807225969            | —             |
| 0.2500000000 | 0.0833466075            | 1.1165815241  |
| 0.1250000000 | 0.0448855064            | 0.8928738060  |
| 0.0625000000 | 0.0240892508            | 0.8978601467  |
| 0.0312500000 | 0.0123820730            | 0.9601366550  |
| 0.0156250000 | 0.0063978976            | 0.9525830630  |

Table 11: Error table for the solution to the Porous Medium Equation (5.3) with  $m = 2$  and the S2 1D scheme.

| $\Delta x$   | $\varepsilon(\Delta x)$ | $o(\Delta x)$ |
|--------------|-------------------------|---------------|
| 0.5000000000 | 0.2737697553            | —             |
| 0.2500000000 | 0.1313948747            | 1.0590540719  |
| 0.1250000000 | 0.0743973715            | 0.8205854463  |
| 0.0625000000 | 0.0417190671            | 0.8345447541  |
| 0.0312500000 | 0.0215359632            | 0.9539590499  |
| 0.0156250000 | 0.0113508296            | 0.9239500977  |

Table 12: Error table for the solution to the Porous Medium Equation (5.3) with  $m = 2$  and the S2 2D scheme.

| $\Delta x$   | $\varepsilon(\Delta x)$ | $o(\Delta x)$ |
|--------------|-------------------------|---------------|
| 0.5000000000 | 0.0433623362            |               |
| 0.2500000000 | 0.0270245038            | 0.6821743579  |
| 0.1250000000 | 0.0068998428            | 1.9696327245  |
| 0.0625000000 | 0.0018979584            | 1.8621151169  |
| 0.0312500000 | 0.0004685419            | 2.0181984180  |
| 0.0156250000 | 0.0001503356            | 1.6399916168  |

Table 13: Error table for the solution to the Porous Medium Equation (5.3) with  $m = 3$  and the S1 1D scheme.

| $\Delta x$   | $\varepsilon(\Delta x)$ | $o(\Delta x)$ |
|--------------|-------------------------|---------------|
| 0.5000000000 | 0.0770913506            |               |
| 0.2500000000 | 0.0453902717            | 0.7641858783  |
| 0.1250000000 | 0.0111666420            | 2.0231877148  |
| 0.0625000000 | 0.0030820998            | 1.8572099249  |
| 0.0312500000 | 0.0007564039            | 2.0266847927  |
| 0.0156250000 | 0.0002419225            | 1.6446120865  |

Table 14: Error table for the solution to the Porous Medium Equation (5.3) with  $m = 3$  and the S1 2D scheme.

| $\Delta x$   | $\varepsilon(\Delta x)$ | $o(\Delta x)$ |
|--------------|-------------------------|---------------|
| 0.5000000000 | 0.0697151007            |               |
| 0.2500000000 | 0.0934099418            | -0.4221049208 |
| 0.1250000000 | 0.0490779933            | 0.9284998456  |
| 0.0625000000 | 0.0198374151            | 1.3068522127  |
| 0.0312500000 | 0.0101275797            | 0.9699346101  |
| 0.0156250000 | 0.0057675969            | 0.8122471959  |

Table 15: Error table for the solution to the Porous Medium Equation (5.3) with  $m = 3$  and the S2 1D scheme.

| $\Delta x$   | $\varepsilon(\Delta x)$ | $o(\Delta x)$ |
|--------------|-------------------------|---------------|
| 0.5000000000 | 0.1055231737            |               |
| 0.2500000000 | 0.1486598990            | -0.4944556727 |
| 0.1250000000 | 0.0821687021            | 0.8553546502  |
| 0.0625000000 | 0.0344059899            | 1.2559292262  |
| 0.0312500000 | 0.0179085612            | 0.9420103138  |
| 0.0156250000 | 0.0102484574            | 0.8052426707  |

Table 16: Error table for the solution to the Porous Medium Equation (5.3) with  $m = 3$  and the S2 2D scheme.

## 5.4 Linear, Nonlinear and Nonlocal Fokker-Planck Equations

In order to validate the order of convergence to a stationary solution we now consider the Linear Fokker-Planck Equation

$$H(\rho) = D(\rho \log(\rho) - \rho), \quad V(\mathbf{x}) = \frac{|\mathbf{x}|^2}{2}, \quad W(\mathbf{x}) = 0, \quad (5.6)$$

for  $D > 0$ . Regardless of the initial data, there is a unique, globally stable steady state for the equation given by the Heat Kernel (5.2) at  $t = 1/2$ , i.e.

$$\rho_\infty(\mathbf{x}) = (2\pi D)^{-\frac{n}{2}} \exp\left(-\frac{|\mathbf{x}|^2}{2D}\right). \quad (5.7)$$

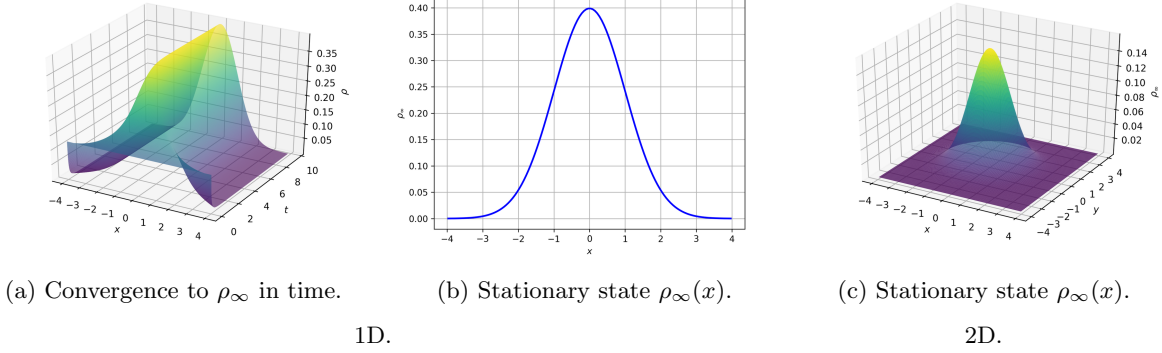


Figure 1: Stationary state of the Nonlocal Fokker-Planck equation (5.8) with  $D = 1$ , equivalent to that of the Linear Fokker-Planck equation (5.6) due to symmetric initial data.

The confining potential of (5.6) can be replaced by an equal interaction potential, allowing for the validation of the interaction component of the schemes. The new equation involves a nonlocal term but will have the same solution as the Linear Fokker-Planck Equation for all initial data which is symmetric about the origin, see Figure 1. This Nonlocal Fokker-Planck Equation

$$H(\rho) = D(\rho \log(\rho) - \rho), \quad V(\mathbf{x}) = 0, \quad W(\mathbf{x}) = \frac{|\mathbf{x}|^2}{2}, \quad (5.8)$$

for  $D > 0$  ought to display the same steady state (5.7) and the same order of convergence to equilibrium as the local case. In the analytic setting, with centered initial data, the  $L_1$  difference  $\|\rho(t, \mathbf{x}) - \rho_\infty(\mathbf{x})\|_{L_1}$  is expected to decay exponentially with order  $\mathcal{O}(-2t)$ . Furthermore, the energy difference  $E(\rho) - E(\rho_\infty)$  should decay with  $\mathcal{O}(-4t)$  [56].

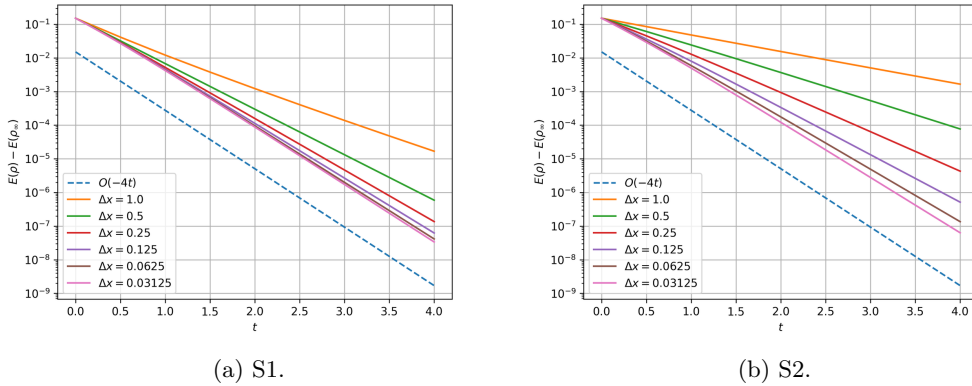


Figure 2: Decay of the discrete energy  $E_\Delta$  in the convergence to the stationary state of the Nonlocal Fokker-Planck equation (5.8) in 2D. Note the slopes approach  $\mathcal{O}(-4t)$  as the mesh is refined,  $\Delta t = \Delta x$ .

We studied the convergence in time of Gaussian initial data in both problems to the numerical steady state, verifying the agreement between the Linear and the Nonlocal settings. Convergence to the known decay rates upon refinement of the mesh was verified as well — see Figure 2 for the 2D case.

To further the discussion we consider a nonlinear diffusion case as well. Replacing the linear term on (5.6) by the Porous Medium setting yields a Nonlinear Fokker-Planck Equation

$$H(\rho) = \frac{D}{m-1}\rho^m, \quad V(\mathbf{x}) = \frac{|\mathbf{x}|^2}{2}, \quad W(\mathbf{x}) = 0, \quad (5.9)$$

for  $D > 0, m > 1$ . Again, regardless of initial data this equation exhibits a globally stable steady state, see Figure 3.

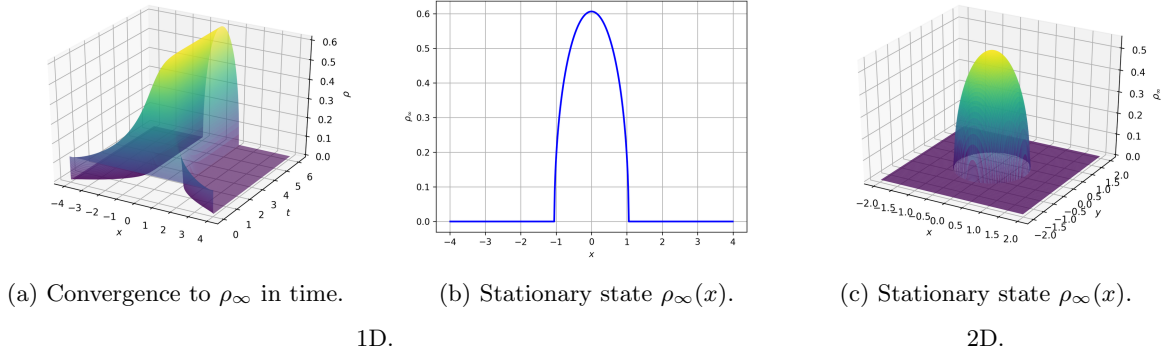


Figure 3: Stationary state of the Nonlinear Fokker Planck equation (5.9) with  $D = 1, m = 3$ .

The regularity of the steady solution is once again controlled by the exponent  $m$ , and so is the rate of convergence to the stationary profile. In 1D, for symmetric initial data, the  $L_1$  difference  $\|\rho(t, \mathbf{x}) - \rho_\infty(\mathbf{x})\|_{L_1}$  and the energy difference  $E(\rho) - E(\rho_\infty)$  decay with  $\mathcal{O}(-(m+1)t)$  and  $\mathcal{O}(-2(m+1)t)$  respectively [26]. Similar verifications were performed — see Figure 4 for the  $m = 3$ .

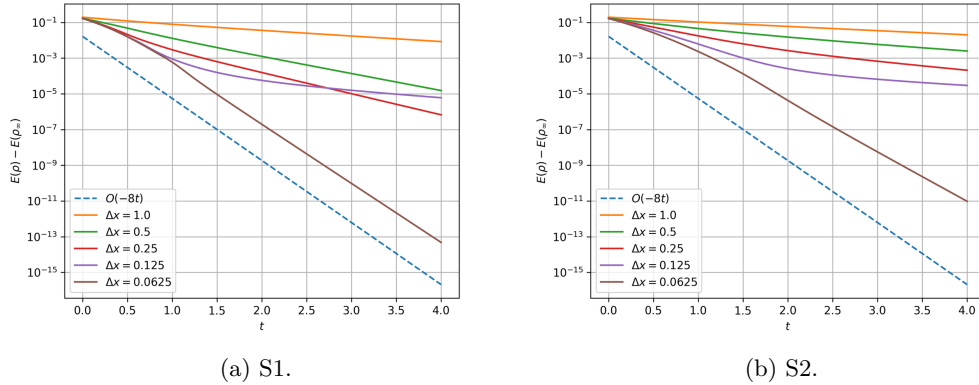


Figure 4: Decay of the discrete energy  $E_\Delta$  in the convergence to the stationary state of the Nonlinear Fokker-Planck equation (5.9) with  $m = 3$  in 1D. Note the slopes approach  $\mathcal{O}(-8t)$  as the mesh is refined,  $\Delta t = \Delta x$ .

## 6 Numerical Experiments

This concluding section presents a selection of experiments which aim to showcase some interesting problems that can be solved with the S2 scheme. First we consider steady state problems with a variety of confining potentials. Later on we discuss equations displaying metastability in the convergence to equilibrium. Finally we study a phase transition driven by noise in a kinetic system by constructing the stable branch of the bifurcation diagram.

### 6.1 Convergence to Steady States

Section 5.4 concerned the convergence to globally stable stationary solutions. Beyond the standard Fokker-Planck setting, the equivalents of (5.6) and (5.9) with more intricate confining potentials may be considered. For instance, a bistable term yields

$$H(\rho) = D(\rho \log(\rho) - \rho), \quad V(\mathbf{x}) = \frac{|\mathbf{x}|^4}{4} - \frac{|\mathbf{x}|^2}{2}, \quad W(\mathbf{x}) = 0, \quad (6.1)$$

for  $D > 0$  in the linear diffusion case, which displays a globally stable steady state characterised by maxima at  $|\mathbf{x}| = 1$  — see Figure 5.

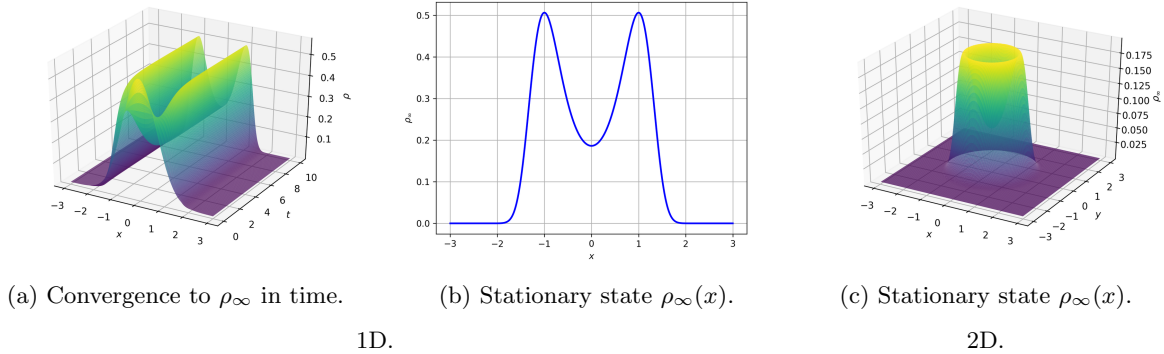


Figure 5: Stationary state of equation (6.1) with  $D = 0.25$ . Note the maxima at  $|\mathbf{x}| = 1$ .

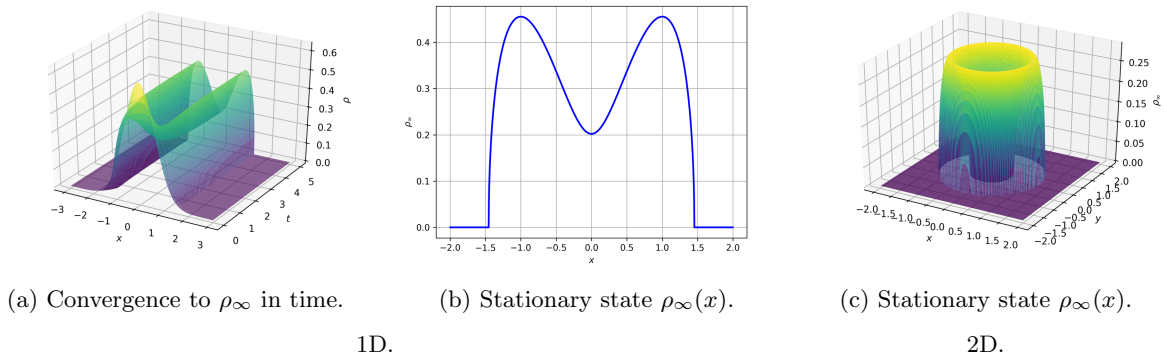


Figure 6: Stationary state of equation (6.2) with  $D = 1, m = 3$ .

In the nonlinear setting, the equation reads:

$$H(\rho) = \frac{D}{m-1} \rho^m, \quad V(\mathbf{x}) = \frac{|\mathbf{x}|^4}{4} - \frac{|\mathbf{x}|^2}{2}, \quad W(\mathbf{x}) = 0, \quad (6.2)$$

for  $D > 0, m > 1$ . The nonlinear diffusion equivalent of (6.1) also has a unique stable steady state, compactly supported and characterised by maxima at  $|\mathbf{x}| = 1$  in 2D. In the 1D setting, the steady state is only unique provided the diffusion coefficient  $D$  is large [20]. Note that in 2D the stationary solution might not be simply connected — see Figure 6.

## 6.2 Metastability

We will now study the behaviour of a nonlinear diffusion equation with an attractive interaction kernel:

$$H(\rho) = \frac{D}{m-1}\rho^m, \quad V(\mathbf{x}) = 0, \quad W(\mathbf{x}) = -e^{-|\mathbf{x}|^2/2\sigma^2}/\sqrt{2\pi\sigma^2}, \quad (6.3)$$

for  $D > 0, m > 1, \sigma > 0$ . This equation can exhibit a many-step convergence to equilibrium: rather than converging at a fixed rate, the energy decays in an alternating sequence of slow and fast timescales. Whilst the true steady state consists of a simply connected, compactly supported component, intermediate aggregates which depend on the initial data can rapidly form. These aggregates will eventually merge but the rate of convergence can be arbitrarily slow if  $\sigma$  is small.

Three examples are presented: Figure 7, where two aggregates are formed before reaching the final equilibrium; Figure 8, where three and then two aggregates are present before the steady state appears; and Figure 9, which shows the asymmetric aggregation in 2D. Note the intermediate plateaux on the energy landscapes, each corresponding to one of the many-aggregate states.

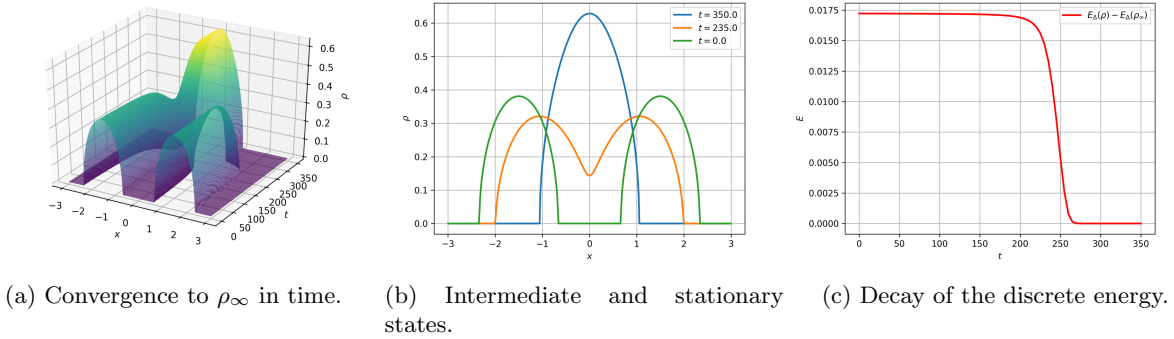


Figure 7: Two-aggregate solution of equation (6.3) for  $D = 0.1, m = 3, \sigma = 0.5$ .

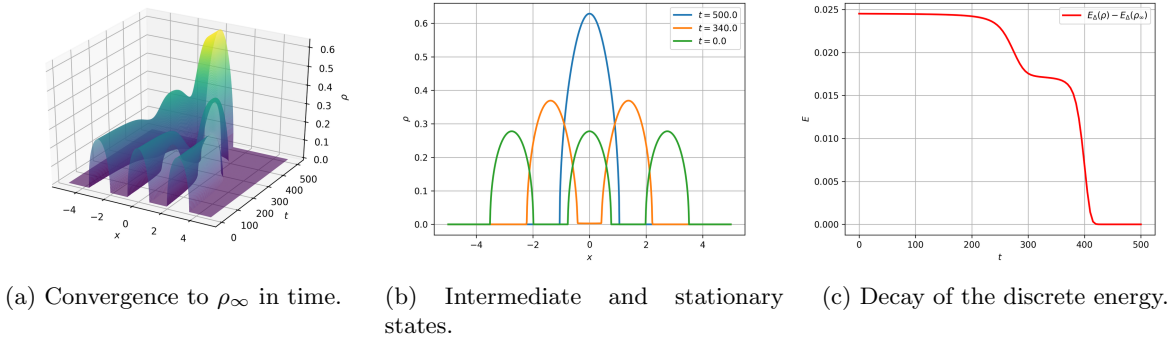
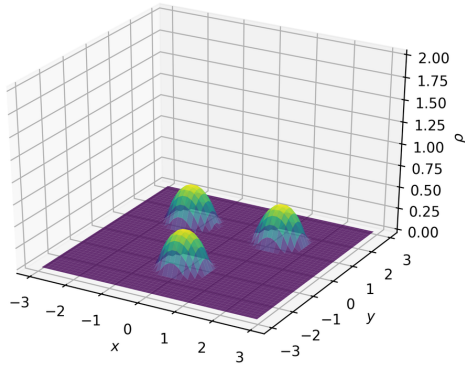
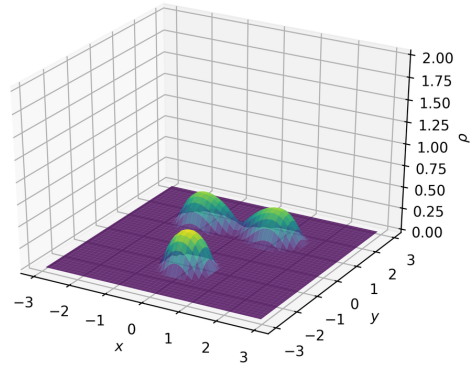


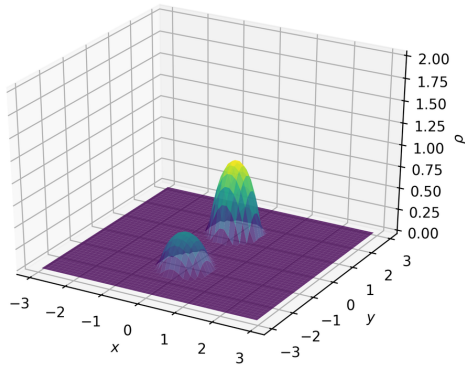
Figure 8: Three-then-two-aggregate solution of equation (6.3) for  $D = 0.1, m = 3, \sigma = 0.5$ .



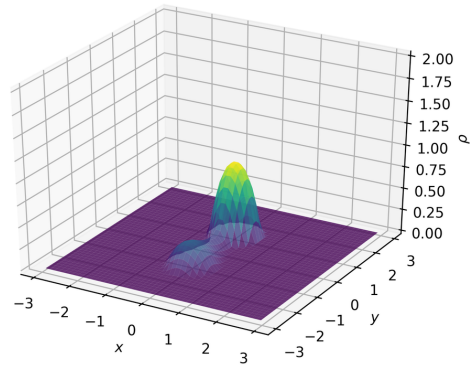
(a)  $t = 0$ .



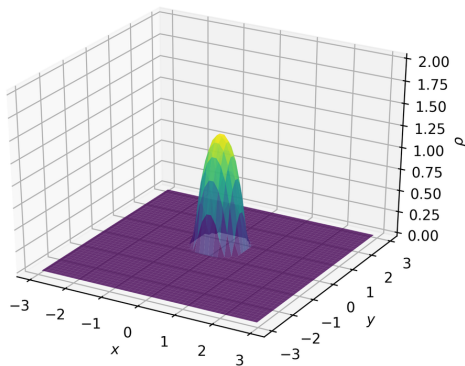
(b)  $t = 150$ .



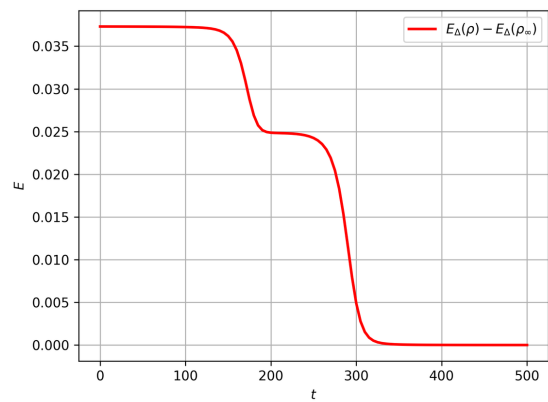
(c)  $t = 230$ .



(d)  $t = 275$ .



(e)  $t = 500$ .



(f) Decay of the discrete energy.

Figure 9: Three-then-two-aggregate solution of equation (6.3) for  $D = 0.01$ ,  $m = 2$ ,  $\sigma = 0.5$  in 2D.

### 6.3 Homogeneous Noisy Kinetic Flocking

For the last example we will discuss a kinetic model for the velocity of self-propelled agents with a noisy tendency to flock:

$$H(\rho) = \sigma(\rho \log(\rho) - \rho), \quad V(\mathbf{x}) = \alpha \left( \frac{|\mathbf{x}|^4}{4} - \frac{|\mathbf{x}|^2}{2} \right), \quad W(\mathbf{x}) = \frac{|\mathbf{x}|^2}{2}, \quad (6.4)$$

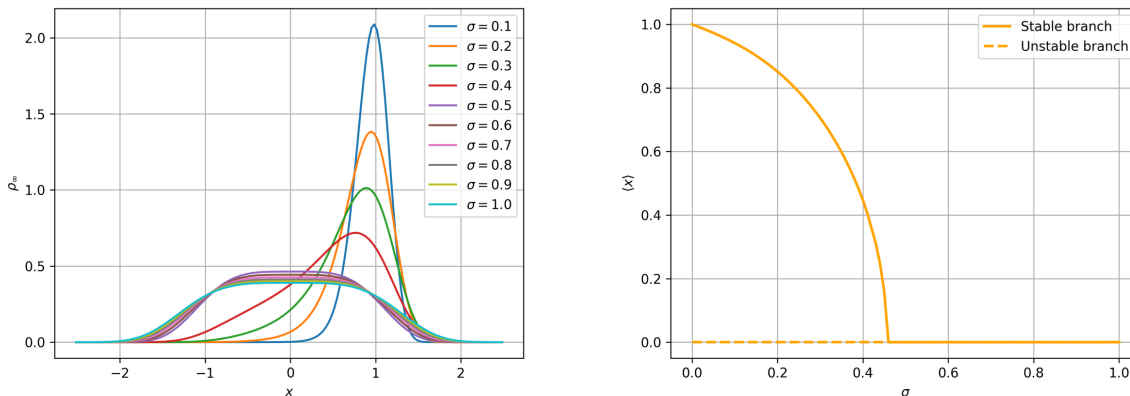
for  $\sigma \geq 0, \alpha \geq 0$ . For the sake of simplicity we retain the notation  $\mathbf{x}$  even though the equation concerns velocities. The confinement potential represents the preference of the agents to move with speed one. The interaction kernel models the alignment tendency, and the diffusion component accounts for the noise in the system.

This model was studied at length in [57, 4, 31]. Among other things, the authors prove the existence of a phase transition in the system. Low values of  $\sigma$  allow asymmetric initial conditions to flock, resulting on polarised steady states; the equation admits a symmetric steady state which is unstable and only realised for symmetric initial data. Increasing the parameter beyond a critical threshold plunges the system into isotropic symmetry regardless of the initial condition.

The S2 scheme allowed us to solve the steady state problem of 6.4 for a large range of values of  $\sigma$ . The first moment of the steady state  $\rho_\infty$ ,

$$\langle \mathbf{x} \rangle = \int \mathbf{x} \rho_\infty d\mathbf{x}, \quad (6.5)$$

can be studied as a function of the noise strength  $\sigma$ , revealing whether the system is polarised or not. A sharp transition from the asymmetric polarised steady states to the isotropic setting can be seen on Figure 10 for the 1D case. The center of mass of the initial data was shifted along the positive axis, resulting on the polarisation in that direction. By symmetry there is always another polarised steady state in the opposite direction.



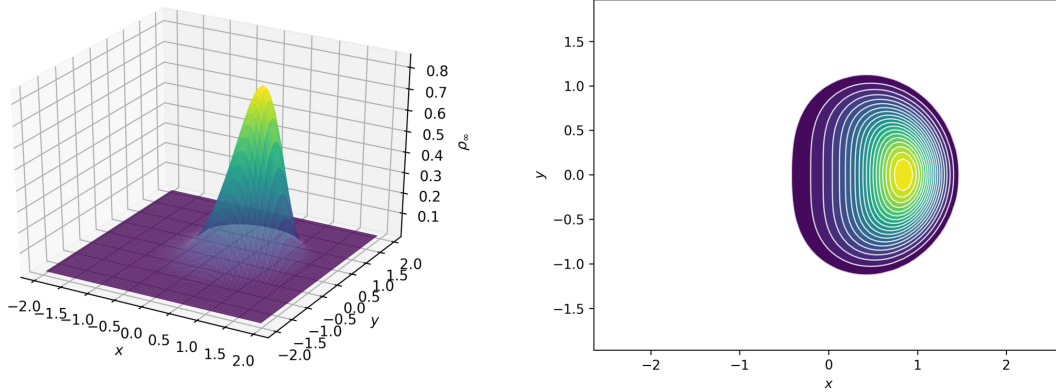
(a) Stationary state  $\rho_\infty(x)$  for different values of  $\sigma$ .

(b) Bifurcation diagram.

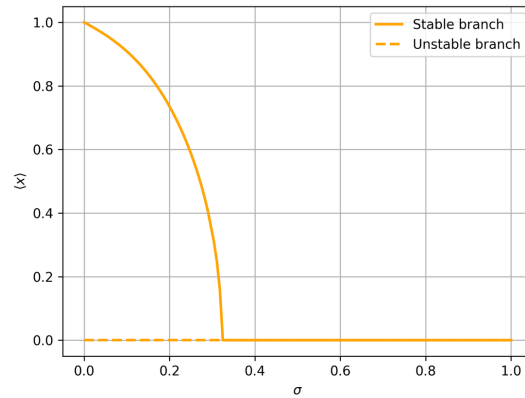
Figure 10: Stationary states and phase transition of (6.4) for  $\alpha = 1$  in 1D.

The same phenomenon is observed in the 2D setting, see Figure 11 and [4] for the analysis. The initial data was shifted along the positive  $x$  axis, resulting on the corresponding polarisation. Note that there is a rotationally symmetric family of polarised steady states. These states resemble a von Mises-Fisher distribution obtained for the Vicsek model ( $\alpha = \infty$ ), see [39].

Finally, we discuss the phase transition for the nonlinear diffusion case with and without a linear



(a) Stationary state  $\rho_\infty(x)$ .



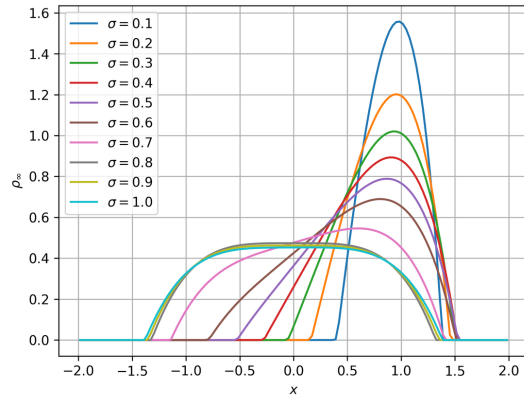
(b) Bifurcation diagram.

Figure 11: Stationary states and phase transition of (6.4) for  $\alpha = 1$  in 2D.

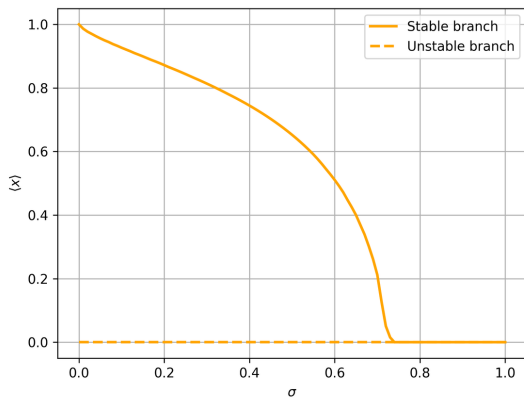
diffusion regularisation. This corresponds to:

$$H_\varepsilon(\rho) = \sigma \left( \frac{\rho^m}{m-1} + \varepsilon(\rho \log(\rho) - \rho) \right), \quad V(\mathbf{x}) = \alpha \left( \frac{|\mathbf{x}|^4}{4} - \frac{|\mathbf{x}|^2}{2} \right), \quad W(\mathbf{x}) = \frac{|\mathbf{x}|^2}{2}, \quad (6.6)$$

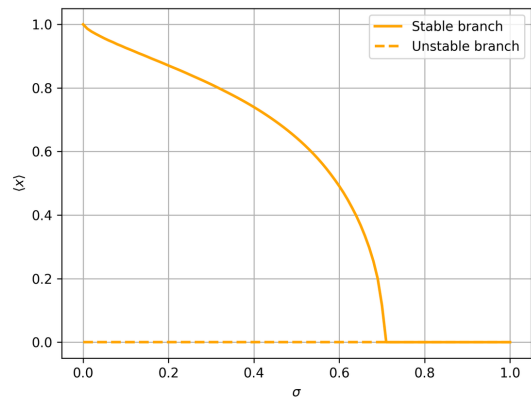
for  $\varepsilon \geq 0, \sigma \geq 0, m > 1, \alpha \geq 0$ . Figure 12 shows the stationary states without regularisation as well as the bifurcation diagrams for  $\varepsilon = 0$  and  $\varepsilon > 0$ . The case shown,  $m = 2$ , leads to compactly supported stationary states with Lipschitz regularity at the boundary of the support, see Figure 12 (a). The regularisation numerically compensates the loss of spatial accuracy of the scheme due to the lack of smoothness of the solution, requiring fewer mesh points to adequately capture the behaviour around the critical point. Numerically we observe that the bifurcation diagram is continuous with respect to the regularisation parameter  $\varepsilon$ .



(a) Stationary states  $\rho_\infty$  for  $H_0(\rho)$  and varying  $\sigma$ .



(b) Bifurcation diagram for  $H_0(\rho)$ .



(c) Bifurcation diagram for  $H_\varepsilon(\rho)$ , with  $\varepsilon = 0.01$ .

Figure 12: Stationary states and phase transition of (6.6) for  $\alpha = 1, m = 2$  in 1D.

## Acknowledgements

JAC was partially supported by the EPSRC grant number EP/P031587/1. JH was supported by NSF grant DMS-1620250 and NSF CAREER grant DMS-1654152. The authors are grateful to the Mittag-Leffler Institute for providing a fruitful working environment during the special semester *Mathematical Biology* where this work was completed. JAC and JH thank the University of Texas at Austin for their invitation in September 2017 where this project started.

## References

- [1] L. N. Almeida, F. Bubba, B. Perthame, and C. Pouchol. Energy and implicit discretization of the fokker-planck and keller-segel type equations. *arXiv preprint arXiv:1803.10629*, 2018.
- [2] L. Ambrosio, N. Gigli, and G. Savaré. *Gradient Flows in Metric Spaces and in the Space of Probability Measures*. Lectures in Mathematics ETH Zürich. Birkhäuser Verlag, Basel, 2008.
- [3] A. Arnold and A. Unterreiter. Entropy decay of discretized Fokker-Planck equations. I. Temporal semidiscretization. *Comput. Math. Appl.*, 46(10-11):1683–1690, 2003.

- [4] A. B. T. Barbaro, J. A. Cañizo, J. A. Carrillo, and P. Degond. Phase transitions in a kinetic flocking model of Cucker-Smale type. *Multiscale Model. Simul.*, 14(3):1063–1088, 2016.
- [5] J. Barré, P. Degond, and E. Zatorska. Kinetic theory of particle interactions mediated by dynamical networks. *Multiscale Model. Simul.*, 15(3):1294–1323, 2017.
- [6] D. Benedetto, E. Caglioti, J. Carrillo, and M. Pulvirenti. A non-Maxwellian steady distribution for one-dimensional granular media. *J. Stat. Phys.*, 91:979–990, 1998.
- [7] D. Benedetto, E. Caglioti, and M. Pulvirenti. A kinetic equation for granular media. *RAIRO Modél. Math. Anal. Numér.*, 31:615–641, 1997.
- [8] M. Bessemoulin-Chatard and F. Filbet. A finite volume scheme for nonlinear degenerate parabolic equations. *SIAM J. Sci. Comput.*, 34(5):B559–B583, 2012.
- [9] J. Bezanson, A. Edelman, S. Karpinski, and V. B. Shah. Julia: A Fresh Approach to Numerical Computing. *SIAM Rev.*, 59(1):65–98, jan 2017.
- [10] A. Blanchet, V. Calvez, and J. A. Carrillo. Convergence of the mass-transport steepest descent scheme for the subcritical Patlak-Keller–Segel model. *SIAM J. Numer. Anal.*, 46(2):691–721, 2008.
- [11] F. Bolley, J. A. Cañizo, and J. A. Carrillo. Stochastic mean-field limit: non-Lipschitz forces and swarming. *Math. Models Methods Appl. Sci.*, 21(11):2179–2210, 2011.
- [12] C. Buet, S. Cordier, and V. Dos Santos. A conservative and entropy scheme for a simplified model of granular media. *Transport Theory Statist. Phys.*, 33(2):125–155, 2004.
- [13] C. Buet and S. Dellacherie. On the Chang and Cooper scheme applied to a linear Fokker-Planck equation. *Commun. Math. Sci.*, 8(4):1079–1090, 2010.
- [14] M. Burger, V. Capasso, and D. Morale. On an aggregation model with long and short range interactions. *Nonlinear Anal. Real World Appl.*, 8(3):939–958, 2007.
- [15] M. Burger, J. A. Carrillo, and M.-T. Wolfram. A mixed finite element method for nonlinear diffusion equations. *Kinet. Relat. Models*, 3(1):59–83, 2010.
- [16] M. Burger, R. Fetecau, and Y. Huang. Stationary states and asymptotic behavior of aggregation models with nonlinear local repulsion. *SIAM J. Appl. Dyn. Syst.*, 13(1):397–424, 2014.
- [17] J. A. Cañizo, J. A. Carrillo, and F. S. Patacchini. Existence of compactly supported global minimisers for the interaction energy. *Arch. Ration. Mech. Anal.*, 217(3):1197–1217, 2015.
- [18] V. Calvez and J. A. Carrillo. Volume effects in the Keller–Segel model: energy estimates preventing blow-up. *J. Math. Pures Appl.*, 86(2):155–175, 2006.
- [19] M. Campos-Pinto, J. A. Carrillo, F. Charles, and Y.-P. Choi. Convergence of a linearly transformed particle method for aggregation equations. *Numerische Mathematik*, 139:743–793, 2018.
- [20] J. A. Carrillo, A. Chertock, and Y. Huang. A finite-volume method for nonlinear nonlocal equations with a gradient flow structure. *Commun. Comput. Phys.*, 17(1):233–258, 2015.
- [21] J. A. Carrillo, A. Colombi, and M. Scianna. Adhesion and volume constraints via nonlocal interactions determine cell organisation and migration profiles. *J. Theoret. Biol.*, 445:75–91, 2018.
- [22] J. A. Carrillo, K. Craig, and F. S. Patacchini. A blob method for diffusion. *arXiv preprint arXiv:1709.09195*, 2017.
- [23] J. A. Carrillo, K. Craig, and Y. Yao. Aggregation-diffusion equations: dynamics, asymptotics, and singular limits. *arXiv preprint arXiv:1810.03634*, 2018.

- [24] J. A. Carrillo, M. G. Delgadino, and A. Mellet. Regularity of local minimizers of the interaction energy via obstacle problems. *Comm. Math. Phys.*, 343(3):747–781, 2016.
- [25] J. A. Carrillo, M. G. Delgadino, and F. Patacchini. Existence of ground states for aggregation-diffusion equations. *to appear in Analysis and Applications, arXiv preprint arXiv:1803.01915*, 2018.
- [26] J. A. Carrillo, M. Di Francesco, and G. Toscani. Strict contractivity of the 2-Wasserstein distance for the porous medium equation by mass-centering. *Proc. Amer. Math. Soc.*, 135(2):353–363, 2007.
- [27] J. A. Carrillo, B. Düring, D. Matthes, and D. S. McCormick. A Lagrangian scheme for the solution of nonlinear diffusion equations using moving simplex meshes. *J. Sci. Comput.*, 75(3):1463–1499, 2018.
- [28] J. A. Carrillo, M. Fornasier, G. Toscani, and F. Vecil. Particle, kinetic, and hydrodynamic models of swarming. In *Mathematical modeling of collective behavior in socio-economic and life sciences*, Model. Simul. Sci. Eng. Technol., pages 297–336. Birkhäuser Boston, Inc., Boston, MA, 2010.
- [29] J. A. Carrillo, M. P. Gualdani, and A. Jüngel. Convergence of an entropic semi-discretization for nonlinear Fokker-Planck equations in  $\mathbb{R}^d$ . *Publ. Mat.*, 52(2):413–433, 2008.
- [30] J. A. Carrillo, R. S. Gvalani, G. A. Pavliotis, and A. Schlichting. Long-time behaviour and phase transitions for the mckean–vlasov equation on the torus. *arXiv preprint arXiv:1806.01719*, 2018.
- [31] J. A. Carrillo, R. S. Gvalani, G. A. Pavliotis, and A. Schlichting. Long-time behaviour and phase transitions for the McKean-Vlasov equation on the torus. pages 1–50, 2018.
- [32] J. A. Carrillo, Y. Huang, and S. Martin. Explicit flock solutions for Quasi-Morse potentials. *European J. Appl. Math.*, 25(5):553–578, 2014.
- [33] J. A. Carrillo, R. J. McCann, and C. Villani. Kinetic equilibration rates for granular media and related equations: entropy dissipation and mass transportation estimates. *Rev. Mat. Iberoamericana*, 19(3):971–1018, 2003.
- [34] J. A. Carrillo and J. S. Moll. Numerical simulation of diffusive and aggregation phenomena in nonlinear continuity equations by evolving diffeomorphisms. *SIAM J. Sci. Comput.*, 31(6):4305–4329, 2009/10.
- [35] J. A. Carrillo, H. Ranetbauer, and M.-T. Wolfram. Numerical simulation of nonlinear continuity equations by evolving diffeomorphisms. *J. Comput. Phys.*, 327:186–202, 2016.
- [36] J. Chang and G. Cooper. A practical difference scheme for fokker-planck equations. *Journal of Computational Physics*, 6(1):1–16, 1970.
- [37] L. Chayes, I. Kim, and Y. Yao. An aggregation equation with degenerate diffusion: qualitative property of solutions. *SIAM J. Math. Anal.*, 45(5):2995–3018, 2013.
- [38] K. Craig and A. L. Bertozzi. A blob method for the aggregation equation. *Math. Comp.*, 85(300):1681–1717, 2016.
- [39] P. Degond, A. Frouvelle, and J.-G. Liu. Phase transitions, hysteresis, and hyperbolicity for self-organized alignment dynamics. *Arch. Ration. Mech. Anal.*, 216(1):63–115, 2015.
- [40] J. Garnier, G. Papanicolaou, and T.-W. Yang. Large deviations for a mean field model of systemic risk. *SIAM J. Financial Math.*, 4(1):151–184, 2013.
- [41] J. Garnier, G. Papanicolaou, and T.-W. Yang. Consensus convergence with stochastic effects. *Vietnam Journal of Mathematics*, 45(1):51–75, Mar 2017.

- [42] S. N. Gomes and G. A. Pavliotis. Mean Field Limits for Interacting Diffusions in a Two-Scale Potential. *J. Nonlinear Sci.*, 28(3):905–941, 2018.
- [43] T. Goudon, S. Jin, and B. Yan. Simulation of fluid-particles flows: heavy particles, flowing regime, and asymptotic-preserving schemes. *Commun. Math. Sci.*, 10(1):355–385, 2012.
- [44] D. D. Holm and V. Putkaradze. Formation of clumps and patches in self-aggregation of finite-size particles. *Phys. D*, 220(2):183–196, 2006.
- [45] O. Junge, D. Matthes, and H. Osberger. A fully discrete variational scheme for solving nonlinear Fokker–Planck equations in multiple space dimensions. *SIAM J. Numer. Anal.*, 55(1):419–443, 2017.
- [46] T. Kolokolnikov, J. A. Carrillo, A. Bertozzi, R. Fetecau, and M. Lewis. Emergent behaviour in multi-particle systems with non-local interactions [Editorial]. *Phys. D*, 260:1–4, 2013.
- [47] P. M. Lushnikov, N. Chen, and M. Alber. Macroscopic dynamics of biological cells interacting via chemotaxis and direct contact. *Phys. Rev. E*, 78:061904, Dec 2008.
- [48] S. Motsch and E. Tadmor. Heterophilious dynamics enhances consensus. *SIAM Rev.*, 56(4):577–621, 2014.
- [49] H. Osberger and D. Matthes. Convergence of a variational Lagrangian scheme for a nonlinear drift diffusion equation. *ESAIM Math. Model. Numer. Anal.*, 48(3):697–726, 2014.
- [50] L. Pareschi and M. Zanella. Structure preserving schemes for nonlinear Fokker-Planck equations and applications. *J. Sci. Comput.*, 74(3):1575–1600, 2018.
- [51] D. Ruelle. *Statistical mechanics: Rigorous results*. W. A. Benjamin, Inc., New York-Amsterdam, 1969.
- [52] J. Shen, J. Xu, and J. Yang. A new class of efficient and robust energy stable schemes for gradient flows. *arXiv preprint arXiv:1710.01331*, 2018.
- [53] Z. Sun, J. A. Carrillo, and C.-W. Shu. A discontinuous Galerkin method for nonlinear parabolic equations and gradient flow problems with interaction potentials. *J. Comput. Phys.*, 352:76–104, 2018.
- [54] A.-S. Sznitman. Topics in propagation of chaos. In *École d’Été de Probabilités de Saint-Flour XIX—1989*, volume 1464 of *Lecture Notes in Math.*, pages 165–251. Springer, Berlin, 1991.
- [55] C. M. Topaz, A. L. Bertozzi, and M. A. Lewis. A nonlocal continuum model for biological aggregation. *Bull. Math. Biol.*, 68:1601–1623, 2006.
- [56] G. Toscani. Entropy production and the rate of convergence to equilibrium for the Fokker-Planck equation. *Quart. Appl. Math.*, 57(3):521–541, 1999.
- [57] J. Tugaut. Phase transitions of McKean-Vlasov processes in double-wells landscape. *Stochastics*, 86(2):257–284, 2014.
- [58] J. L. Vazquez. *The Porous Medium Equation*. Oxford University Press, oct 2006.
- [59] C. Villani. *Topics in optimal transportation*, volume 58 of *Graduate Studies in Mathematics*. American Mathematical Society, Providence, RI, 2003.